History of anthropogenic Nitrogen inputs (HaNi) to the terrestrial biosphere: A 5-arcmin resolution annual dataset from 1860 to 2019

Hanqin Tian[1,2]*, Zihao Bian[2,1]*, Hao Shi[3,2]*, Xiaoyu Qin[3], Naiqing Pan[2,1], Chaoqun Lu[4], Shufen Pan[2,1], Francesco N. Tubiello[5], Jinfeng Chang[6], Giulia Conchedda[5], Junguo Liu[7], Nathaniel Mueller[8,9], Kazuya Nishina[10], Rongting Xu[11], Jia Yang[12], Liangzhi You[13], Bowen Zhang[14]

[1]Schiller Institute for Integrated Science and Society, Department of Earth and Environmental Sciences, Boston College, Chestnut Hill, MA 02467, USA;[2]International Center for Climate and Global Change Research and College of Forestry, Wildlife and Environment, Auburn University, Auburn, AL 36849, USA; [3]Research Center for Eco-Environmental Sciences, State Key Laboratory of Urban and Regional Ecology, Chinese Academy of Sciences, Beijing 100085, China; [4]Department of Ecology, Evolution, and Organismal Biology, Iowa State University, Ames, IA 50011, USA; [5]Statistics Division, Food and Agriculture Organization of the United Nations, Via Terme di Caracalla, Rome, Italy; [6]College of Environmental and Resource Sciences, Zhejiang University, Hangzhou 310058, China; [7]School of Environmental Science and Engineering, Southern University of Science and Technology, Shenzhen 518055, China.[8]Department of Ecosystem Science and Sustainability, Colorado State University, Fort Collins, CO 80523, USA;[9]Department of Soil and Crop Sciences, Colorado State University, Fort Collins, CO 80523, USA; [10]Biogeochemical Cycle Modeling and Analysis Section, Earth System Division, National Institute for Environmental Studies 16-2, Onogawa, Tsukuba, 305-8506, JAPAN; [11]Forest Ecosystems and Society, Oregon State University, Corvallis, OR 97330, USA; [12]Department of Natural Resource Ecology and Management, Oklahoma State University, Stillwater, OK 74078, USA;[13]International Food Policy Research Institute (IFPRI), 1201 Eye Street, NW, Washington, DC 20005, USA; [14]Department of Environment, Geology, and Natural Resources, Ball State University, Muncie, IN 47306, USA

Corresponding authors:

Hanqin Tian (hanqin.tian@bc.edu);

Zihao Bian (zzb0009@auburn.edu);

Hao Shi (haoshi@rcees.ac.cn)

Abstract

30 Excessive anthropogenic nitrogen (N) inputs to the biosphere have disrupted the global nitrogen

31 cycle. To better quantify the spatial and temporal patterns of anthropogenic N enrichments, assess

32 their impacts on the biogeochemical cycles of the planet and other living organisms, and improve

33 nitrogen use efficiency (NUE) for sustainable development, we have developed a comprehensive

34 and synthetic dataset for reconstructing the History of anthropogenic N inputs (HaNi) to the

35 terrestrial biosphere. The HaNi dataset takes advantage of different data sources in a

36 spatiotemporally consistent way to generate a set of high-resolution gridded N input products from

37 the preindustrial to present (1860-2019). The HaNi dataset includes annual rates of synthetic N

38 fertilizer, manure application/deposition, and atmospheric N deposition in cropland, pasture, and

39 rangeland at a spatial resolution of 5-arcmin. Specifically, the N inputs are categorized, according

40 to the N forms and land uses, as ten types: 1) NH_4^+-N fertilizer applied to cropland, 2) NO_3-N

41 fertilizer applied to cropland, 3) NH_4^+-N fertilizer applied to pasture, 4) NO_3-N fertilizer applied

42 to pasture, 5) manure N application on cropland, 6) manure N application on pasture, 7) manure

43 N deposition on pasture, 8) manure N deposition on rangeland, 9) NH_x-N deposition, and 10) NO_y-

44 N deposition. The total anthropogenic N (TN) inputs to global terrestrial ecosystems increased

45 from 29.05 Tg N yr^{-1} in the 1860s to 267.23 Tg N yr^{-1} in the 2010s, with the dominant N source

46 changing from atmospheric N deposition (before the 1900s) to manure N (the 1910s-2000s), and

47 to synthetic fertilizer in the 2010s. The proportion of synthetic NH_4^+-N fertilizer increased from

48 64% in the 1960s to 90% in the 2010s, while synthetic NO_3-N fertilizer decreased from 36% in

49 the 1960s to 10% in the 2010s. Hotspots of TN inputs shifted from Europe and North America to

50 East and South Asia during the 1960s-2010s. Such spatial and temporal dynamics captured by the

51 HaNi dataset are expected to facilitate a comprehensive assessment of the coupled human-earth

52 system and address a variety of social welfare issues, such as climate-biosphere feedback, air

53 pollution, water quality, and biodiversity. Datasets are available at

54 https://doi.org/10.1594/PANGAEA.942069 (Tian et al., 2022).

55

56

57

1. Introduction

Nitrogen (N) is an essential element for the survival of all living organisms, required by various biological molecules, for instance, nucleic acids, proteins, and chlorophyll (Galloway et al., 2021; Schlesinger and Bernhardt, 2020). Most N on the Earth is not readily available for organisms, since it either exists in the form of inert N_2 gas or is stored in crust and sediments (Ward, 2012). Driven by the human demand for food and energy, a spectrum of approaches has been developed to produce biologically available N (Sutton et al., 2013; Lassaletta et al. 2016), ranging from traditional methods, such as legume crops cultivation and manure application, to modern techniques, such as industrial compost and the Haber-Bosch process that produce organic fertilizer mixture and chemical fertilizer, respectively. Increasing anthropogenic N inputs have significantly boosted crop yield and improved food security (Stewart and Roberts, 2012), but also resulted in over twofold increase in terrestrial reactive N (Galloway and Cowling 2002; Fowler et al. 2013; Melillo, 2021; Scheer et al., 2020) and are expected to continually increase in the coming decades due to human demand for food (Kanter et al. 2020; Sutton et al. 2021).

The large amount of excessive reactive N in terrestrial ecosystems has led to multiple environmental issues like water quality deterioration, air pollution, global warming, and biodiversity loss (Bouwman et al., 2005; Gruber and Galloway, 2008; Howarth, 2008; Pan et al., 2021; Tian et al., 2020a; Vitousek et al., 1997). The river export of various forms of nitrogen (ammonium, nitrate, dissolved organic N) has largely increased (Schlesinger et al., 2006; Tian et al., 2020b), frequently causing large-scale hypoxia along coastal oceans for example, in the northern Gulf of Mexico (Bargu et al., 2019; Dodds, 2006; Rabalais and Turner, 2019). The global emission of ammonia (NH_3), a major precursor of aerosols contributing to air pollution, had rapidly increased from 1.0 Tg N yr^{-1} in 1961 to 9.9 Tg yr^{-1} in 2010, mainly due to the wide use of N fertilizer (Xu et al., 2019a). The emissions of nitrous oxide (N_2O), the third most important greenhouse gas, had increased by 30% over the past four decades, which was mainly attributed to N addition to croplands (Cui et al., 2021; Tian et al., 2020a; Wang et al., 2020). Moreover, excessive usage of N over other nutrients (e.g. phosphorus) brings nutrient imbalance that may induce significant alterations in the structure and functions of ecosystems and finally result in losses of biodiversity (Galloway et al., 2003; Lun et al., 2018; Peñuelas and Sardans, 2022; Houlton et al., 2019).

88 In light of the critical impacts of N excess on the human-earth system, numerous efforts have been
89 conducted to generate distribution maps of N inputs for different sectors with varied temporal
90 coverage and spatial resolution (Potter et al., 2010; Nishina et al., 2017; Bian et al., 2021; Liu et
91 al., 2010). Country-level N fertilizer data from the Food and Agriculture Organization of the
92 United Nations (FAO) and the International Fertilizer Association (IFA) have been widely used to
93 assess global and national nitrogen budgets for crop production (Xiong et al., 2008; Zhang et al.,
94 2021b; Eickhout et al., 2006). However, spatial variations of N inputs within countries have been
95 overlooked in country-level data, while detailed geospatial distributions of N inputs are required
96 for many process-based modeling studies (Tian et al., 2019, 2018). Potter et al. (2010) and Mueller
97 et al. (2012) both generated crop-specific spatially-explicit N fertilizer data which, however,
98 represented the average fertilizer application patterns around 2000. Liu et al. (2010) developed a
99 N balance model, and made the first attempt to quantify six N inputs (e.g. mineral fertilizer, manure,
100 atmospheric deposition, biological fixation, input from sedimentation, and input from recycled
101 crop residual) and five N outputs (e.g. output to harvested crops, crop residues, leaching, gaseous
102 losses, and soil erosion) in cropland for the year 2000 with a spatial resolution of 5-arcmin. Lu and
103 Tian (2017) created an annual dataset of global N fertilizer application in cropland at a spatial
104 resolution of $0.5° \times 0.5°$ during 1961-2013, and Nishina et al. (2017) further split synthetic N
105 fertilizer application into NH_4^+ and NO_3^- forms. Meanwhile, Zhang et al. (2017) reconstructed
106 global manure N production and application rates in cropland which covered the period 1860-2014
107 and had a resolution of 5-arcmin; using a similar methodology, Xu et al., (2019b) further developed
108 three gridded datasets, i.e., rangeland manure deposition, pasture manure deposition, and pasture
109 manure application, all of which had a resolution of $0.5° \times 0.5°$ and spanned from 1860-2016.
110 Although these datasets are valuable in addressing their respective objective issues, there is a
111 barrier in taking advantage of them simultaneously, due to the inconsistent temporal coverage,
112 spatial resolution, data sources (e.g., N inputs statistics and land use), and spatial allocation
113 algorithms. Therefore, the reconstruction for the History of Anthropogenic N Inputs (HaNi) to the
114 terrestrial biosphere with rich spatial details and long-term coverage is essentially needed.

115 To address this issue, using sophisticated methodologies, we employed multiple statistical data,
116 empirical estimates, atmospheric chemistry model outputs (Eyring et al., 2013), and high-
117 resolution land-use products to generate the HaNi dataset. This comprehensive dataset consists of
118 N fertilizer/manure application to cropland, manure application/deposition to pasture, manure

119 deposition to rangeland, and atmospheric N deposition on all agricultural land at a resolution of 5-
120 arcmin from 1860 to 2019. Additionally, we tried to investigate the impacts of social-economic
121 forcing on N use across different regions. These efforts are anticipated to benefit understanding
122 the spatial and temporal patterns of human-induced N enrichment, assessing impacts of excessive
123 N on global and regional biogeochemical cycles, and providing data support for resource
124 management. The HaNi dataset has also been expected to serve as input data for Earth system
125 models, biogeochemical models, and hydrological models for improving our understanding and
126 assessment of global consequences of anthropogenic nitrogen enrichment for climate change, air
127 and water quality, ecosystems, and biodiversity (e.g. Tian et al., 2018).

2. Methods

2.1. Data sources of fertilizer/manure use

130 Multiple anthropogenic N input databases were integrated to generate the HaNi dataset (Table 1).
131 For the period of 1961-2019, annual country-level statistics data was obtained from the FAOSTAT
132 "Land, Inputs and Sustainability" domain (FAO, 2021). "N fertilizer applied to soil" was from the
133 "Fertilizers by Nutrient" subsection. "Manure applied to soil" and "Manure left on pasture" data
134 were from the "Livestock Manure" subsection. Before 1961, the time series of fertilizer and
135 manure use from Holland et al. (2005) was adopted and corrected to be consistent with FAO
136 statistics. For countries (e.g., the former Soviet Union, the Socialist Federal Republic of
137 Yugoslavia, Eritrea, Ethiopia, and the Czechoslovak Republic) that experienced political
138 disintegration, we partitioned their pre-disintegration N fertilizer/manure use into each individual
139 new-formed country using the ratios derived from the N uses of the new-formed countries in the
140 first year after disintegration.

141 The FAOSTAT agricultural use of N fertilizer and manure referred to the N use for crops, livestock,
142 forestry, fisheries, and aquaculture, excluding N use for animal feed. Since the use of N fertilizers
143 and manure for forestry, fisheries, and aquaculture was minor compared to that for crops and
144 livestock, this part was taken as negligible. The partitioning ratio of N fertilizer application to
145 cropland and pasture was adopted from Lassaletta et al. (2014). Since Lassaletta's ratio values only
146 covered the period of 1961-2009, values in 2009 were used to calculate the N application
147 partitioning after 2009. By FAO's definition, manure applied to soil was equal to the difference
148 between all treated manure and N loss during stored and treated processes. Therefore, we assumed

149 that the total quantity of manure applied to soil was equal to the total quantity of manure applied
150 to cropland and pasture. The fraction values for cropland were from Zhang et al. (2015), who
151 assumed the fraction value ranged between 0.5 and 0.87 for European countries, Canada, and the
152 U.S., while it was 0.9 for other countries.

153 Table 1. Summary of main data sources

Data Source	Dataset	Reference
FAOSTAT	Annual country-level fertilizer and manure inputs to land from 1961 to 2019	FAO (2021)
EARTHSTAT	Fertilizer and manure application rates for major crops	(Mueller et al., 2012) (West et al., 2014)
EARTHSTAT	Harvested area and yield for major crops	(Monfreda et al., 2008)
Hyde3.2/LUHv2	Cropland, Pasture, and rangeland area from 1860 to 2019	(Klein Goldewijk et al., 2017) (Hurtt et al., 2020)
Holland et al., 2005	Global fertilizer and manure N from 1860 to 1960	(Holland et al., 2005)
Nishina et al., 2017	Annual NH4 and NO3 fraction in total fertilizer from 1961 to 2014	(Nishina et al., 2017)
GLW3	Livestock distribution maps	(Gilbert et al., 2018)
Eyring et al. 2013	Monthly atmospheric N depositions (NHx-N and NOy-N) during 1850–2014	(Eyring et al., 2013)

154

155

2.2 Land use data

The HYDE3.2 dataset (Klein Goldewijk et al., 2017) provides historical spatial distributions of
cropland, pasture, and rangeland at a 5-arcmin resolution and at an annual time-step after 2000 but
a decadal time-step before the 1990s. In contrast, the LUHv2 dataset (Hurtt et al., 2020), derived
mainly from HYDE3.2, has an annual time-step across 1860-2019 but at a relatively low spatial
resolution of $0.25° \times 0.25°$. To reconcile these two datasets, we first conducted a linear
interpolation to HYDE3.2 before 1999 using the data of every two neighbor decades. Then the
fraction of crop/pasture/rangeland of a LUHv2 grid was partitioned into all grid cells of HYDE3.2
that fell in the LUHv2 grid, according to their shares in HYDE3.2. Through this routine, we
obtained a land-use dataset that both kept spatial information of HYDE3.2 and was consistent with
LUHv2 on the total area for each land use type.

2.3 Spatializing N fertilizer and manure application in cropland

The workflow of spatializing the country-level N fertilizer and manure use amount to gridded maps is shown in Fig 1. First, the grid-level crop-specific N fertilizer and manure use rates per cropland area of 17 dominant crop types (wheat, maize, rice, barley, millet, sorghum, soybean, sunflower, potato, cassava, sugarcane, sugar beet, oil palm, rapeseed, groundnut, cotton, and rye), which were developed by Mueller et al. (2012) and West et al. (2014), were combined with the crop-specific harvested area (Monfreda et al. 2008) to generate baseline distribution maps circa 2000 of fertilizer and manure application in cropland. The crop-area-based average N fertilizer and manure rates in each grid cell (at a resolution of 5-arcmin) were calculated as:

$$\overline{C_{fer/man}} = \frac{\sum_i (C_{fer/man,i} \times AH_i)}{\sum_i AH_i} \tag{1}$$

where $\overline{C_{fer/man}}$ is the area-weighted average of N fertilizer or manure application rates (i.e., gridded baseline fertilizer or manure application rate, in the unit of g N m^{-2} cropland yr^{-1}). $C_{fer/man,i}$ and AH_i are crop-specific N fertilizer or manure application rate (g N m^{-2}) and harvested area (m^2), respectively, for crop type i.

Second, we used annual country-level N fertilizer and manure application amounts from FAO (1961-2019) and the annual cropland area to scale the baseline year 2000 maps of N fertilizer and manure application rates across time using the following equation:

$$R_{fer/man,y,j} = \frac{FAO_{fer/man,y,j}}{\sum_{g=1}^{g=n\ in\ country\ j} (\overline{C_{fer/man}} \times AC_{y,g})} \tag{2}$$

where $R_{fer/man,y,j}$ is the regulation ratio (unitless) in the year y and country j. $FAO_{fer/man,y,j}$ is country-level total N fertilizer or manure use amount (g N yr^{-1}) on cropland derived from FAOSTAT. $AC_{y,g}$ is the area of cropland (m^2) derived from the historical land use data in the year y and grid g. The actual N fertilizer and manure application rates were then calculated using the following equation:

$$N_{fer/man} = \overline{C_{fer/man}} \times R_{fer/man,y} \tag{3}$$

where $N_{fer/man}$ is the "real" gridded N fertilizer or manure use rates (g N m^{-2} cropland yr^{-1}) in the year y.

Then, we extended the fertilizer data back to 1925 and manure data back to 1860 using the global N flux change rates (Holland et al. 2005). Since industrial production of synthetic fertilizer was developed in the early 1910s, we further extend fertilizer data back by assuming the fertilizer production linearly increased from 1910 to 1925. Finally, N fertilizer application in cropland was further divided into the NH_4^+ form the NO_3^- form based on the annual country-level NH_4^+ application ratio in total N fertilizer provided by Nishina et al. (2017). This data was estimated based on FAOSTAT's consumption data by chemical fertilizer type, which takes into account the NH_4^+ and NO_3^- content in each fertilizer type individually.
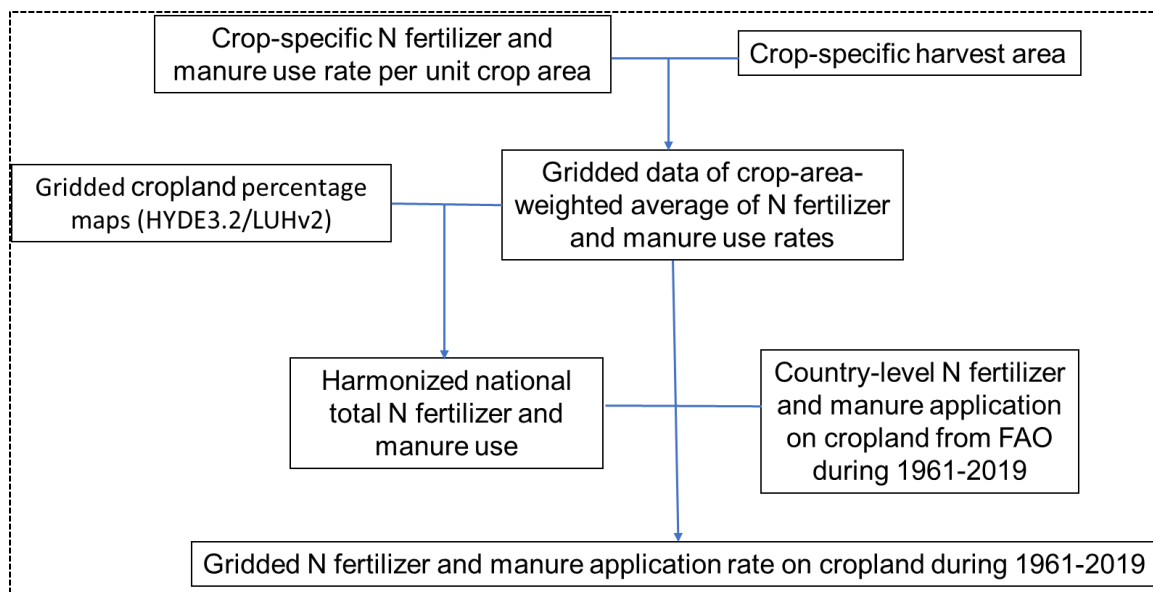
Figure 1. The workflow for developing the dataset of global annual N fertilizer and manure application rates during 1961-2019.

2.4. Spatializing the total fertilizer and manure N in pasture and rangeland

2.4.1. N fertilizer use in pasture

Due to the lack of grid-level spatial information of N fertilizer use in pasture, we assumed that pasture within each country has an even annual N fertilizer use rate. The fertilizer use in pasture per country was divided by the total pasture area of that country. Then this N fertilizer use rate per country was assigned to all the pasture grid cells in that country (Fig 2). The detailed method was introduced in Xu et al. (2019b).

213
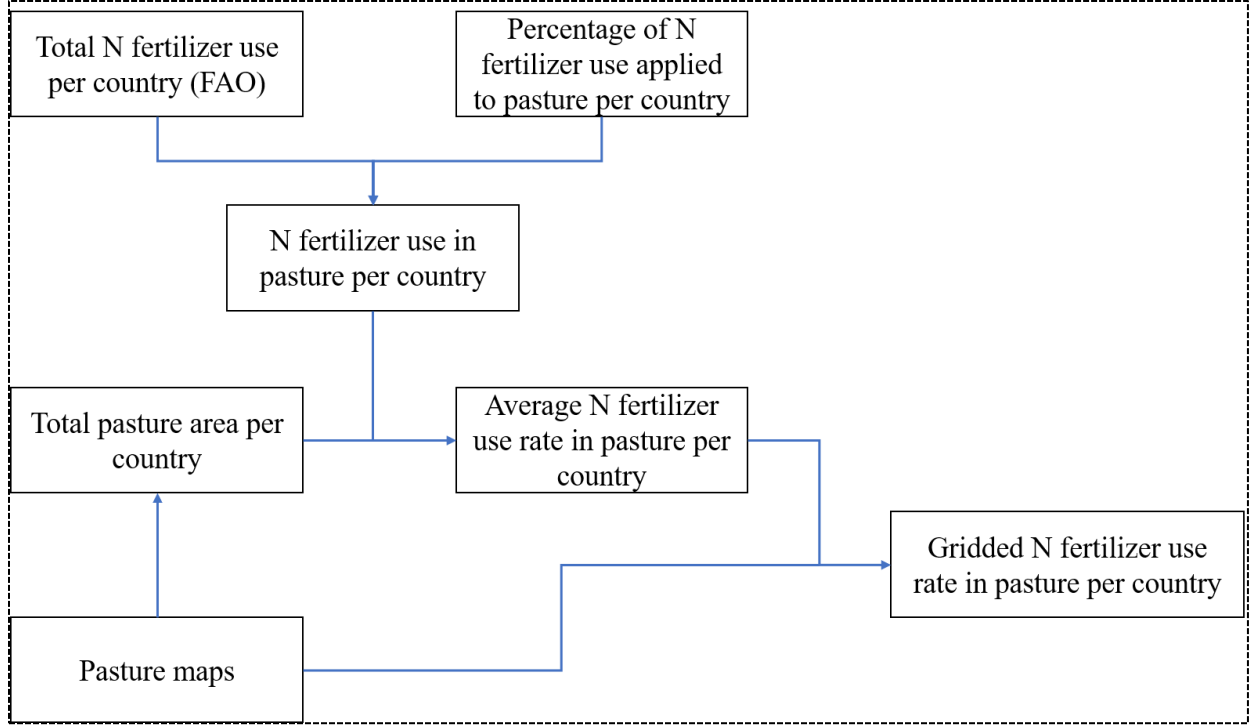
Figure 2. The workflow for developing the global pasture fertilizer application rate data during
1961-2019.

2.4.2. Spatializing manure application in pasture

To generate spatial patterns of manure application in pasture, we first calculated the spatial
distribution of annual manure N production. The Global Livestock of World 3 database (GLW3;
Gilbert et al., 2018) was used as a reference map of livestock distribution, which provided spatial
information for buffaloes, cattle, chickens, ducks, horses, goats, pigs, and sheep at a spatial
resolution of 0.083° in 2010. For the period 1961-2019, the FAO statistics of livestock population
in a country in one year was compared with the sum of GLW3 grid values within that country and
the ratio of the two values was used to scale all the GLW3 grid values of the country to generate
the spatial distribution of livestock in that year (Fig. 3). This routine can be represented as:

$$D_{l,c,y}^{FAO} = D_{l,c}^{GLW3} \times \frac{T_{l,c,y}^{FAO}}{T_{l,c}^{GLW3}} \qquad (4)$$

where $T_{l,c,y}^{FAO}$ indicates the FAO statistics of the population of the lth type of livestock of country c
in year y, $T_{l,c}^{GLW3}$ indicates the national population of the lth type of livestock of country c
summarized from GLW3, $D_{l,c}^{GLW3}$ is the spatial distribution corresponding to $T_{l,c}^{GLW3}$, and $D_{l,c,y}^{FAO}$ is

229 the corresponding spatial distribution to $T_{l,c,y}^{FAO}$. Applying the IPCC Tier 1 methodology for N

230 excretion (Dong et al., 2006) to these derived spatial distribution maps of livestock, we can have

231 the spatial maps of annual manure production during 1961-2019. Specifically, the average daily N

232 excretion rate was different for each livestock and for each group of countries, which were

233 classified by socioeconomic and geographic conditions. All manure production data were

234 resampled to 5-arcmin to be consistent with the pasture land use data.

235 Manure application to pasture during 1961-2019 is then estimated using manure production and

236 pasture area (Fig. 3) as:

237
$$R_{c,y}^{Napp/Nprod} = \frac{Napp_{c,y}^{FAO}}{sum(GNprod_{c,y}^{FAO} \times GParea_{c,y}^{LU})} \tag{5}$$

238
$$GNapp_{c,y}^{FAO} = mask(R_{c,y}^{Napp/Nprod} \times GNprod_{c,y}^{FAO}, GParea_{c,y}^{LU}) \tag{6}$$

239 where $R_{c,y}^{Napp/Nprod}$ is the ratio of FAO statistics of manure application to pasture in country c in

240 year y ($Napp_{c,y}^{FAO}$) over the estimated manure production in the same country and the same year,

241 $GNprod_{c,y}^{FAO}$ is the gridded manure production in country c in year y estimated based on FAO

242 statistics of livestock data, $GParea_{c,y}^{LU}$ is the gridded pasture area in country c in year y from our

243 land use data, and $GNapp_{c,y}^{FAO}$ is the corresponding gridded manure application to pasture in

244 country c in year y through masking the product raster of $R_{c,y}^{Napp/Nprod}$ and $GNprod_{c,y}^{FAO}$ by the

245 $GParea_{c,y}^{LU}$ raster. The manure application to pasture in year y during 1860-1960 was estimated as

246 the product of $GNprod_{c,y}^{Holland}$ and $R_{c,1961}^{Napp/Nprod}$ (Fig 3). As for the period 1860-1960, the time

247 series of manure application data were also generated according to the manure N change rates

248 derived from Holland et al. (2005).

249
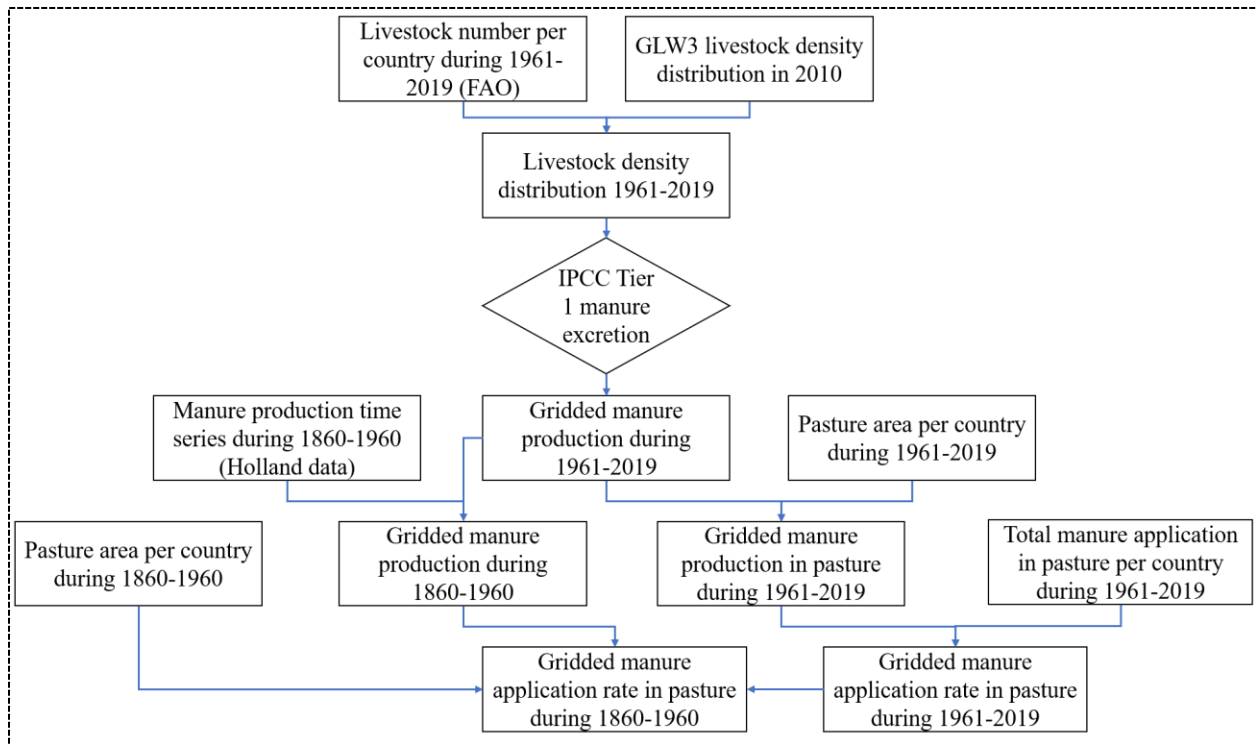
Figure 3. The workflow for developing the global pasture manure application rate data during 1860-2019.

250
251

252

2.4.3. Spatializing manure deposition in pasture and rangeland

253

The routine for spatializing FAO statistics of manure deposition on pasture and rangeland was similar to the method for manure deposition to pasture in Xu et al. (2019b). The only difference is that the manure deposition intensity on pasture was assumed to be twice that on rangeland within a grid cell, according to previous research (Campbell and Stafford Smith, 2000). To avoid inconsistencies between total manure use and total manure production within a grid cell and unrealistic transport distances, the sum of manure application to cropland and pasture and manure deposition to pasture and rangeland was constrained to be less than or equal to manure production within a grid cell. In fact, the case that the total manure use surpassed the total manure production in a grid cell was rare. If there was, the four components, namely the manure application to cropland and pasture and manure deposition to pasture or rangeland, were scaled by multiplying the ratio of their sum over the total manure production within a grid cell.

2.5 Atmospheric nitrogen deposition

Monthly atmospheric N depositions (NH_x-N and NO_y-N) during 1850–2014 were from N deposition fields of model simulations in the International Global Atmospheric Chemistry (IGAC)/Stratospheric Processes and Their Role in Climate (SPARC) Chemistry–Climate Model Initiative (CCMI) (Morgenstern et al., 2017). For the period 2015-2020, N deposition under SSP585 (the highest emission scenario in shared socio-economic pathways) was used, consistent with Dynamic Global Vegetation Model simulations (TRENDY) for the global carbon budget (Friedlingstein et al., 2020). The CCMI models considered N emissions from multiple sources, including anthropogenic and biofuel sources, natural biogenic sources, biomass burning and lightning, and the transport of N gases and wet/dry N deposition (Eyring et al., 2013). The CCMI N deposition data was developed in support of the Coupled Model Intercomparison Project Phase 6 (CMIP6) and used as the official products for CMIP6 models that lack interactive chemistry components. The nearest interpolation method was used to resample N deposition data to a spatial resolution of 5-arcmin.

2.6 Regional Analysis

In order to compare anthropogenic N inputs across different regions, we divided the global land area into 18 regions according to national or continental boundaries (Tian et al. 2019). The 18 regions are USA, Canada (CAN), Central America (CAM), Northern South America (NSA), Brazil (BRA), Southwest South America (SSA), Europe (EU), Northern Africa (NAF), Equatorial Africa (EQAF), Southern Africa (SAF), Russia (RUS), Central Asia (CAS), Middle East (MIDE), China (CHN), Korea and Japan (KAJ), South Asia (SAS), Southeast Asia (SEAS), and Oceania (OCE).

3. Results

3.1. Temporal and spatial changes in total anthropogenic N inputs

The total anthropogenic N (TN) inputs to global terrestrial ecosystems increased from 29.05 Tg N yr^{-1} in the 1860s to 267.23 Tg N yr^{-1} in the 2010s (Fig 4 and Table 2). The most rapid increase of total N inputs was 3.53 Tg N yr^{-2} occurred during 1945-1990 driven by both elevated fertilizer application rates and cropland expansion. The TN inputs leveled off within the 1990s, but increased again after 2001 with a lower increasing rate though. The TN inputs were dominated by atmospheric N deposition before the 1900s. Manure N kept an increasing trend, accounting for

more than half of the TN inputs from the 1910s to the 1960s. Thereafter, the proportion of N fertilizer in TN inputs substantially increased from 15% in the 1960s to 39 % in the 2010s, meanwhile, the proportions of manure N and atmospheric N deposition decreased from 54% and 31% to 37% and 24%, respectively.

Table 2. Decadal average of N inputs into the terrestrial ecosystem (Tg N yr^{-1})

Decade	Nfer NH$_4$ Crop	Nfer NO$_3$ Crop	Nfer NH$_4$ Pas	Nfer NO$_3$ Pas	Nman App Crop	Nman App Pas	Nman Dep Pas	Nman Dep Ran	Ndep NH$_x$	Ndep NO$_y$	Total
1860s	0.00	0.00	0.00	0.00	2.52	1.01	3.92	2.04	10.32	9.24	29.05
1910s	0.08	0.05	0.00	0.00	6.54	2.20	9.87	6.38	11.59	10.72	47.43
1960s	11.81	5.98	0.19	0.12	14.86	3.60	26.99	20.77	20.15	18.35	122.80
1970s	28.21	12.09	1.21	0.72	17.23	4.14	30.77	23.17	25.40	22.98	165.94
1980s	47.27	16.98	2.97	1.67	19.46	4.54	34.22	24.49	31.90	27.34	210.83
1990s	56.42	14.59	4.02	1.73	20.19	4.29	36.99	25.67	33.80	28.55	226.26
2000s	70.32	10.57	5.77	1.33	20.66	4.01	39.57	27.50	33.45	28.73	241.91
2010s	87.52	9.03	7.39	1.10	22.29	4.09	43.25	28.68	35.58	28.30	267.23

Note: Nfer—N fertilizer, Nman—manure N, Ndep—N deposition, Crop—Cropland, Pas—Pasture, Ran—Rangeland, App—Application, Dep—Deposition.
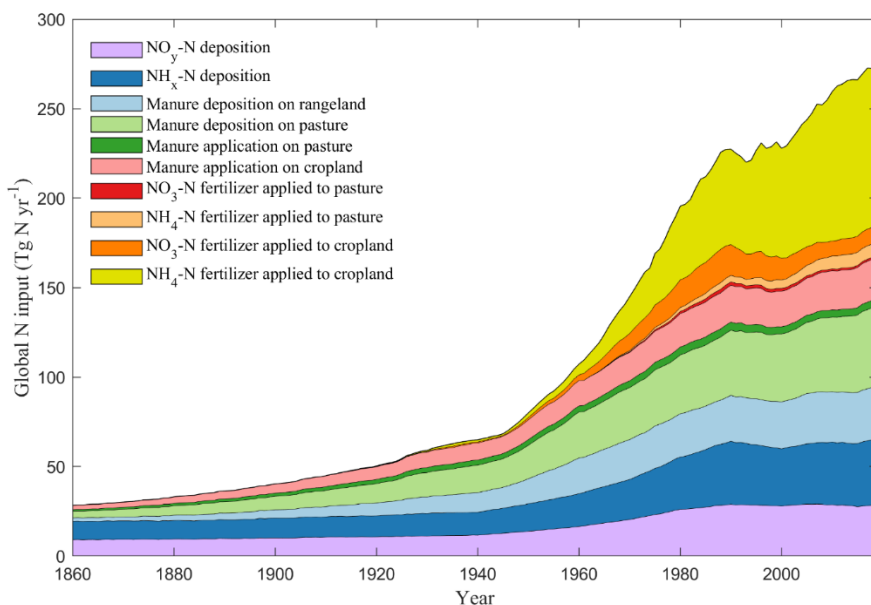
Figure 4. Long-term trends of anthropogenic nitrogen inputs to terrestrial ecosystems during 1860-2019. N input to global terrestrial ecosystems from three major categories: N fertilizer, manure N, and N deposition, which are further divided into ten specific types, including NH$_4$-N fertilizer applied to cropland, NO$_3$-N fertilizer applied to cropland, NH$_4$-N fertilizer applied to pasture, NO$_3$-N fertilizer applied to pasture, manure N application on cropland, manure N application on pasture,

309 manure N deposition on pasture, manure N deposition on rangeland, NH_x-N deposition, and NO_y-
310 N deposition.

311

312 The TN inputs exhibited high spatial heterogeneity across the globe, associated with the
313 imbalances in regional economic development and population growth (Fig. 5). From the 1860s to
314 the 1910s, the TN inputs mainly increased in the eastern U.S., Europe, and India, driven by the
315 increase in manure N application and deposition. In the 1960s, several hotspots of the TN inputs
316 emerged in Europe (Fig. 5c) where synthetic fertilizer was first widely used. Meanwhile, the TN
317 inputs were also intensified in many regions of the developing countries, such as eastern China,
318 southern Brazil, India, and countries in central Africa, mainly due to the increasing use of manure
319 N (Fig. 5c). As the access to the synthetic N fertilizer became easier, the TN inputs significantly
320 increased across the globe from the 1960s to the 2010s, and the inter-regional imbalance of N
321 inputs had also been amplified, with regions of high N inputs concentrated in eastern and central
322 China, India, Europe, midwestern U.S., and southern Brazil (Fig. 5d).
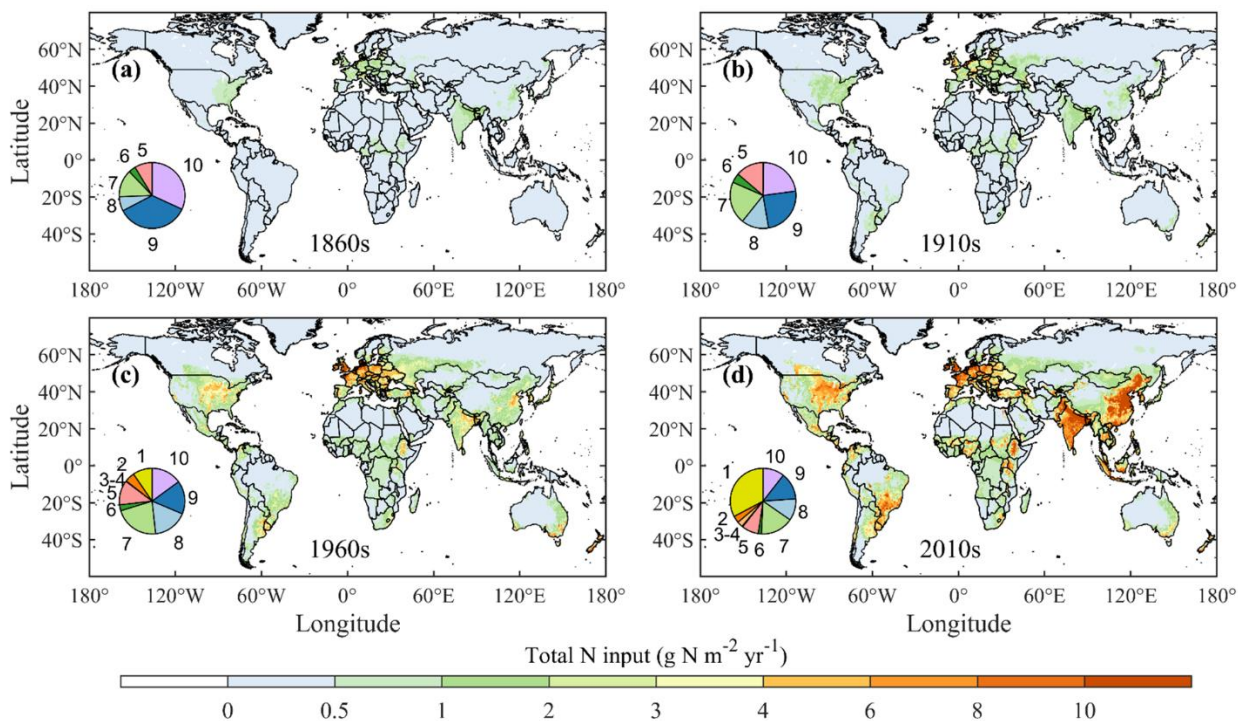
323

324 **Figure 5.** Spatial patterns of total N input in the (a) 1860s, (b) 1910s, (c) 1960s, and (d) 2010s.
325 For the pie chart in the spatial map, the numbers 1-10 represent the percentage of each component,
326 respectively (1. 'NH4-N fertilizer applied to cropland', 2. 'NO3-N fertilizer applied to cropland',
327 3. 'NH4-N fertilizer applied to pasture', 4. 'NO3-N fertilizer applied to pasture', 5. 'Manure

328 application on cropland', 6. 'Manure application on pasture', 7. 'Manure deposition on pasture',
329 8. 'Manure deposition on rangeland', 9. 'NHx-N deposition', 10. 'NOy-N deposition').

330

331 Among the 18 regions (Fig 6), the top three regions with the highest TN inputs in 1960 were
332 Europe (19.0 Tg N yr^{-1}), USA (11.8 Tg N yr^{-1}), and South Asia (9.9 Tg N yr^{-1}). From 1960 to 2019,
333 the largest increases in TN inputs were found in China, South Asia, and Brazil, which accounted
334 for 26%, 18%, and 9% of the increase of the global N inputs, respectively. The increasing TN
335 inputs in China and South Asia were mainly driven by the wide use of synthetic fertilizer, while
336 those in Brazil were driven by the use of both livestock manure and synthetic fertilizer. The TN
337 inputs in USA became relatively stable since 1980, whereas the TN inputs in Europe decreased by
338 32% from 1988 to 2019, primarily due to the increase in crop N use efficiency and the reduction
339 in synthetic fertilizer application (Zhang et al., 2021a; Lassaletta et al., 2014). Although the TN
340 inputs in China experienced a rapid increase in recent decades, it started to show a decreasing trend
341 after 2014. However, the TN inputs in South Asia and Brazil continued maintaining a strong
342 growth trend. In 2019, China (49.1 Tg N yr^{-1}) contributed the largest share (18%) to global TN
343 inputs, followed by South Asia (38.9 Tg N yr^{-1}, 14%) and Europe (26.2 Tg N yr^{-1}, 10%). The TN
344 inputs in North America (USA and CAN), Europe (EU), East and South Asia (CHN, KAJ, SAS,
345 and SFAS) were dominated by synthetic fertilizer, while those in Central and South America (BRA,
346 SSA, NSA, and CAM), Africa (NAF, EQAF, and SAF), Central and West Asia (CAS and MIDE),
347 and Oceania (OCE) were dominated by manure. RUS was the only region where atmospheric N
348 deposition was the major anthropogenic N source in 2019.
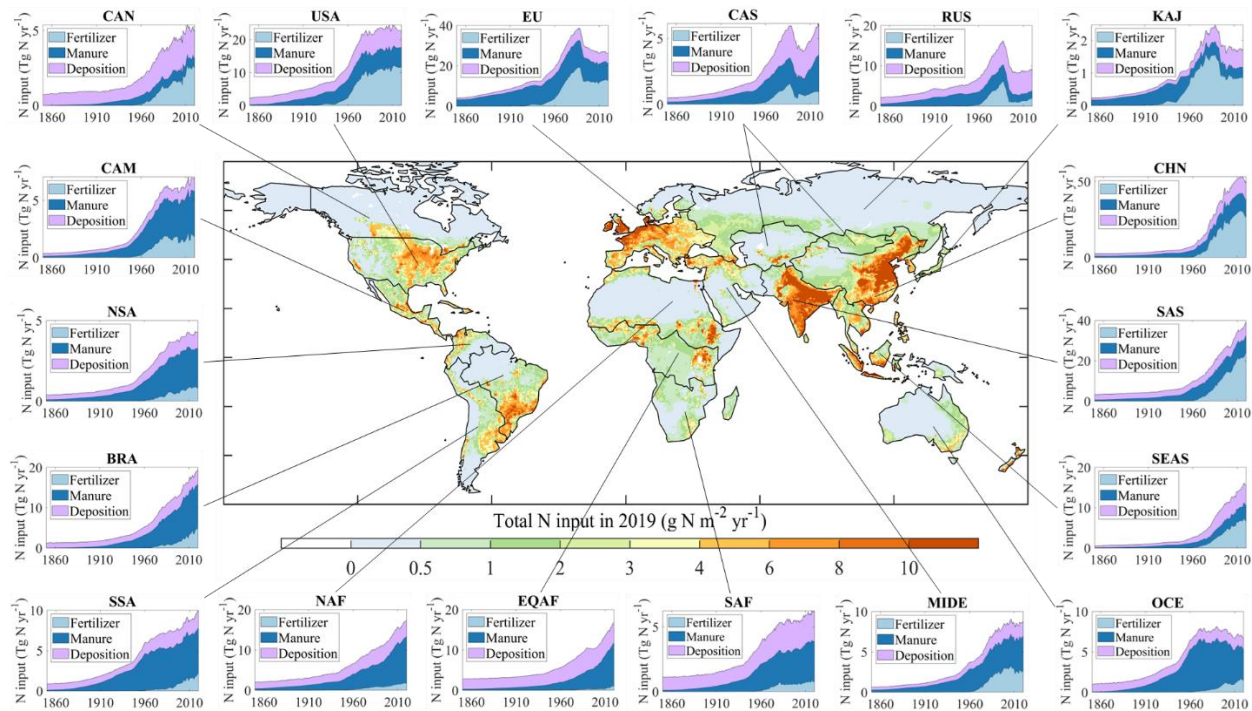
Figure 6. Long-term trends and variations of regional N inputs (synthetic fertilizer, livestock manure, and atmospheric deposition) to terrestrial ecosystems during 1860-2019. The 18 regions are USA, Canada (CAN), Central America (CAM), Northern South America (NSA), Brazil (BRA), Southwest South America (SSA), Europe (EU), Northern Africa (NAF), Equatorial Africa (EQAF), Southern Africa (SAF), Russia (RUS), Central Asia (CAS), Middle East (MIDE), China (CHN), Korea and Japan (KAJ), South Asia (SAS), Southeast Asia (SEAS), and Oceania (OCE).

3.2. N fertilizer inputs on cropland and pasture

From the 1960s to the 2010s, the N fertilizer inputs on cropland and pasture increased from 18.1 Tg N yr^{-1} to 105.0 Tg N yr^{-1}. Specifically, N fertilizer inputs on cropland increased from 17.8 Tg N yr^{-1} to 96.6 Tg N yr^{-1}, and N fertilizer inputs on pasture increased from 0.3 Tg N yr^{-1} to 8.5 Tg N yr^{-1} (Fig. 4 and Table 2). The proportion of NH_4^+ fertilizer in N fertilizer increased from 64% in the 1960s to 90% in the 2010s, contrarily NO_3^--N fertilizer decreased from 36% in the 1960s to 10% in the 2010s. At the regional level, Europe and USA were the top two N fertilizer-consuming regions in the 1960s, accounting for 38% and 25% of global N fertilizer application, while China (28%) and South Asia (21%) were the top two in the 2010s (Fig. 6). Fertilizer

366   application rates in China and South Asia increased at a rate of 0.59 Tg N yr^{-2} and 0.43 Tg N yr^{-2}

367   (p<0.05) during 1960-2019, respectively.
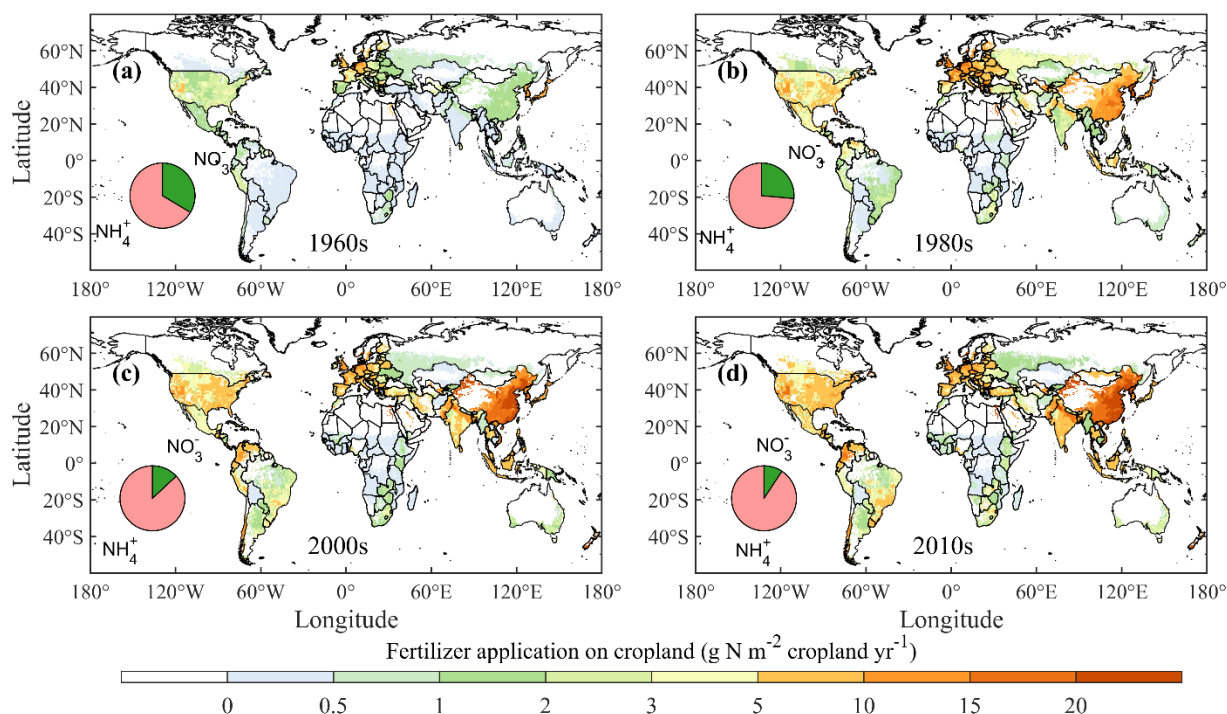
369   **Figure 7.** Spatial patterns of N fertilizer application on cropland in the 1960s, 1980s, 2000s, and
370   2010s.

372   Fertilizer application rates on cropland in Europe reached the maximum in the 1980s, but fertilizer

373   application rates in India, eastern Asia, and southern Brazil kept increasing continuously (Fig 7).

374   In the 2010s, extremely high N fertilizer inputs (> 20.0 g N m^{-2} yr^{-1}) mainly occurred in eastern

375   and southeastern China. Croplands in northern India and western Europe also had high N fertilizer

376   rates (> 10.0 g N m^{-2} yr^{-1}). N fertilizer application changed slowly in Africa, with most croplands

377   receiving N fertilizer less than 2.0 g N m^{-2} yr^{-1}. For pasture, Europe was the main region with N

378   fertilizer application over 6.0 g N m^{-2} yr^{-1} before the 1980s (Fig. S1). N fertilizer application on

379   pasture in southern Canada and India increased significantly with rates over 8.0 g N m^{-2} yr^{-1} in the

380   2010s. Most other regions (e.g., China, U.S., Brazil, Africa) received N fertilizer application of

381   less than 3.0 g N m^{-2} yr^{-1}.

3.3. Manure N inputs on cropland, pasture, and rangeland

The total manure N inputs to land increased from 9.48 Tg N yr^{-1} in the 1860s to 98.31 Tg N yr^{-1} in the 2010s, with an increasing rate of 0.6 Tg N yr^{-2} (Fig 4 and Table 2). The manure N application on cropland, manure application on pasture, manure deposition on pasture, and manure deposition on rangeland changed from 14.86 Tg N yr^{-1} (22% of total manure input), 3.60 Tg N yr^{-1} (5%), 26.99 Tg N yr^{-1} (41%), and 20.77 Tg N yr^{-1} (31%) in the 1960s to 22.29 Tg N yr^{-1} (23%), 4.09 Tg N yr^{-1} (4%), 43.25 Tg N yr^{-1} (44%), and 28.68 Tg N yr^{-1} (29%) in the 2010s, respectively. Europe was the largest contributor (39%) to global manure N inputs in the 1860s, but its share decreased in the last century and became 9% in the 2010s (Fig. 6). The manure N inputs in Brazil grew rapidly from 0.55 Tg N yr^{-1} (2% of global manure N inputs) in the 1910s to 10.77 Tg N yr^{-1} (11%) in the 2010s. Similarly, manure N inputs in Equatorial Africa and Northern Africa were only 2.22 Tg N yr^{-1} (3%) and 4.20 Tg N yr^{-1} (6%) in the 1960s and increased dramatically to 9.40 Tg N yr^{-1} (10%) and 10.60 Tg N yr^{-1} (11%) in the 2010s, respectively. China was the largest contributor (12%) of global total manure N inputs in the 2010s, while it contributed 8% in the 1960s and 12% in the 1860s.
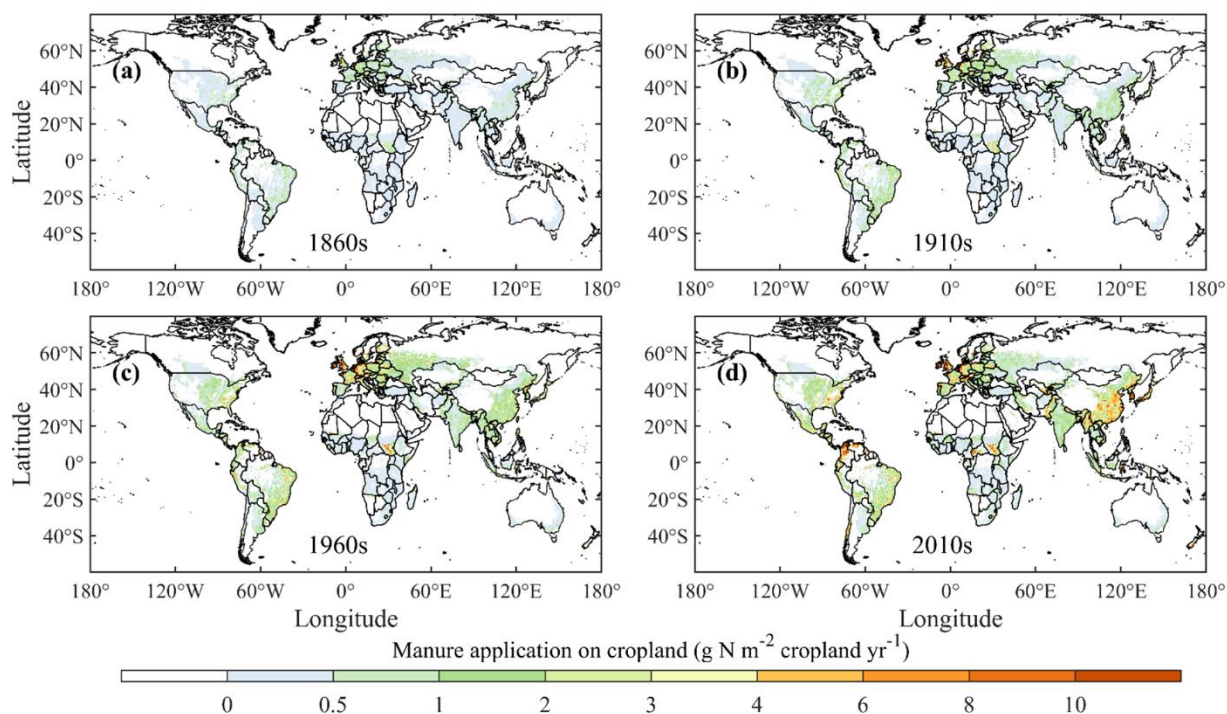
Figure 8. Spatial patterns of manure N application on cropland in the 1860s, 1910s, 1960s, and 2010s.

Manure application rates on cropland gradually intensified across the globe since the 1860s except in Australia and part of Africa (Fig. 8). Hotspots of manure application on cropland (> 6.0 g N m^{-2} yr^{-1}) first appeared in western Europe in the 1910s, then intensified manure application was observed in eastern Asia and northern South America in the 2010s. Manure application and deposition on pasture had higher spatial variability than that on cropland (Fig. 9). Pasture in Europe and South Asia received higher manure N than that in other regions. Eastern South America, central Africa, and eastern Asia also experienced a significant increase in manure N inputs on pasture since the 1910s. For manure deposition on rangeland, South Asia stood out over the study period, with several other hotspots emerging in central Africa, northern China, Europe, and eastern South America since the 1910s (Fig 10).
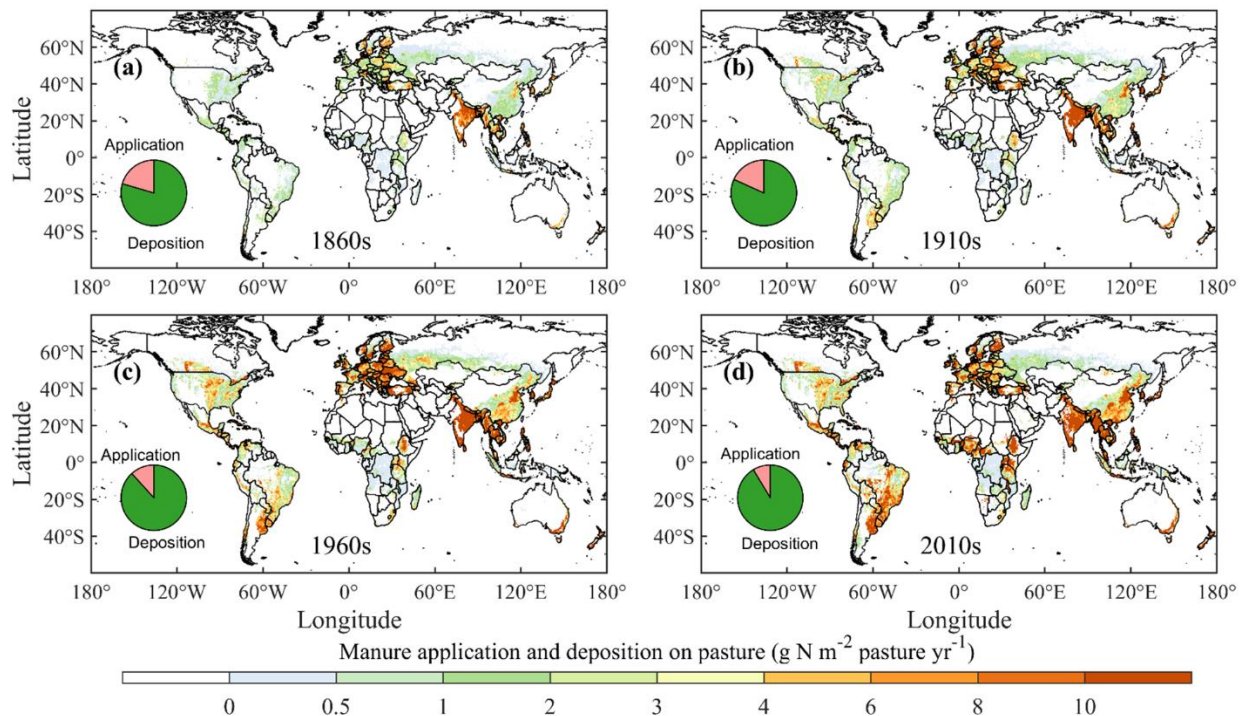
Figure 9. Spatial patterns of manure N application and deposition on pasture in the 1860s, 1910s, 1960s, and 2010s.
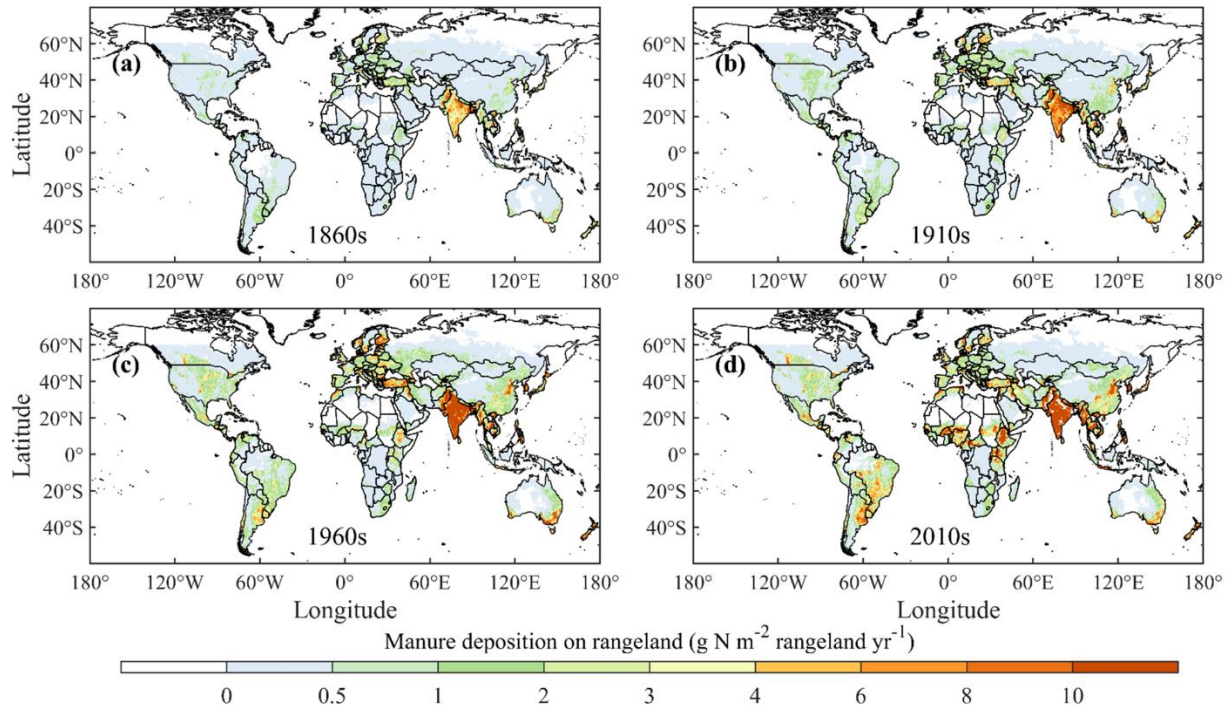
Figure 10. Spatial patterns of manure N deposition on rangeland in the 1860s, 1910s, 1960s, and 2010s.

3.4. Atmospheric N deposition on land

Atmospheric N deposition has a threefold increase from 19.06 Tg N yr^{-1} to 60.87 Tg N yr^{-1} during the 1850s - the 2010s, with NH$_x$ deposition increasing from 10.02 Tg N yr^{-1} to 35.58 Tg N yr^{-1} and NO$_y$ deposition increasing from 9.04 Tg N yr^{-1} to 28.30 Tg N yr^{-1} (Fig 4 and Table 2). The share of NH$_x$ in atmospheric N deposition started to increase after the 1970s, changing from 52% to 56% in the 2010s. At the regional scale, South Asia, Equatorial Africa, and USA were the largest contributors in the 1860s, accounting for 13%, 13%, and 12% of global atmospheric N deposition, respectively (Fig 6). In the 2010s, China was the region with the largest atmospheric N deposition (10.66 Tg N yr^{-1}, 17% of global atmospheric N deposition), followed by South Asia (5.90 Tg N yr^{-1}, 9%) and USA (5.69 Tg N yr^{-1}, 9%). Atmospheric N deposition peaked in the 1980s in Europe and Equatorial Africa, the 1990s in USA, and the 2010s in South Asia and China. Spatially, atmospheric N deposition intensified and increased dramatically across the globe since the 1910s (Fig. 11), and regions with high N deposition rates (>1.0 g N m^{-2} yr^{-1}) were mainly in Europe, central Africa, southern Asia, U.S. (since the 1960s), and eastern Asia (in the 2010s).
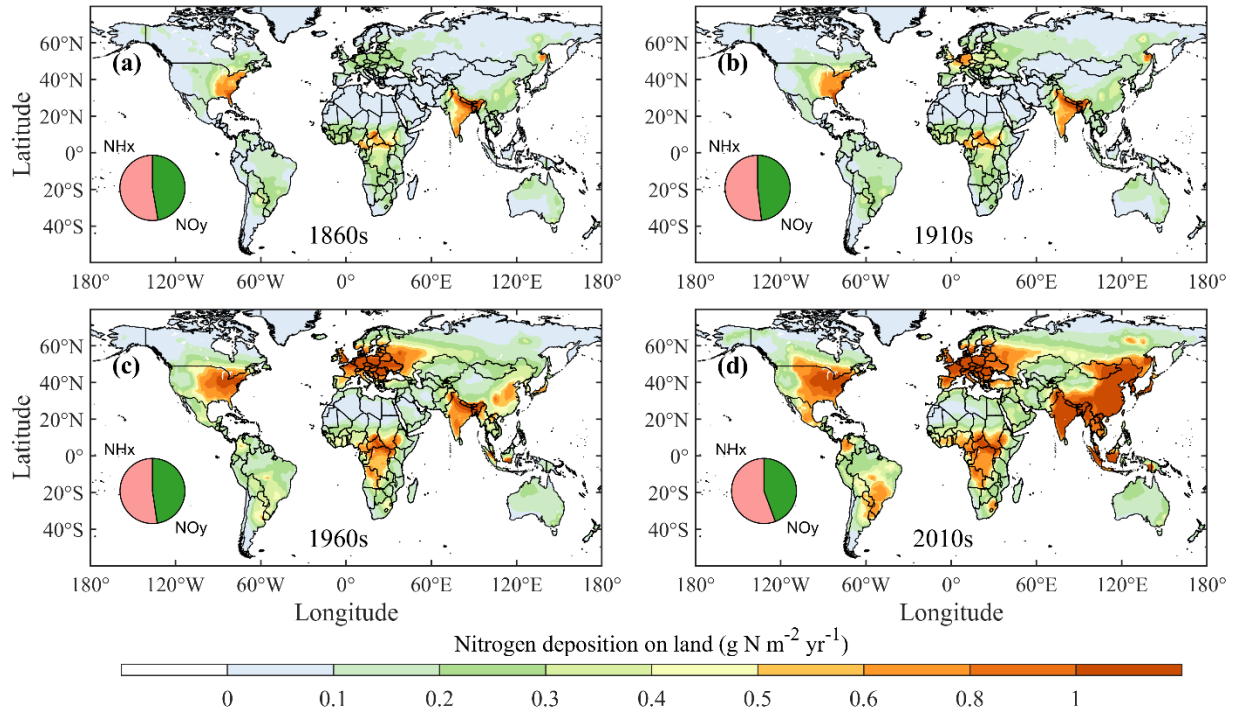
Figure 11. Spatial patterns of atmospheric N deposition on land in the 1860s, 1910s, 1960s, and 2010s.

4. Discussion

4.1 Socioeconomic forcing of N use

The total anthropogenic nitrogen inputs (excluding N deposition) showed a close relationship with GDP per capita in all the three agricultural sectors of cropland, pasture, and rangeland (Fig. 12). These relationships could be generally categorized into three groups: a hump-shaped curve, a rapid increase curve, and an asymptote curve. The first was typically seen in regions like China and Europe. China, as the top N consumer, has successfully reduced its nitrogen use for crop production from the peak of 33.6 Tg yr^{-1} in 2014 to 30.0 Tg yr^{-1} in 2020. Crop production in China increased in the same period due to the improvements in crop varieties, fertilizer management, and land use policies (Cui et al., 2018; Wu et al., 2018). The mandatory policies and directives for N use in Europe since the late 1980s have effectively curbed its N use to a stable level (Van Grinsven et al., 2014). The second could be seen in South Asia, Southeast Asia, North Africa, etc. These regions are still in the developing stage and need to tackle the food demand of rapidly growing population, which, together with low nitrogen use efficiency, results in a surge of nitrogen

453   pollution (Chang et al., 2021). The third could be well represented by USA and Canada. For the

454   USA, although its crop nitrogen use efficiency has considerably improved since the 1990s driven

455   by technological and management improvements (Zhang et al., 2015), its cropland area has kept

456   expanding recently with the new cropland usually producing yields below the national average

457   (Lark et al., 2020), which undermines its efforts for reducing N excess induced environmental

458   pollution. For the same curve type, there also existed obvious differences. For example, the turning

459   points for crop N inputs in Europe and China emerged at varied socioeconomic development levels.

460   Meanwhile, it was difficult to predict when China's crop N inputs would decrease to its lowest as

461   Europe's case had shown. For different sectors of one country or region, their N inputs could also

462   show asynchrony with GDP per capita increases. Take the USA as an instance, its N inputs on

463   cropland and pasture kept growing while its N inputs on rangeland had kept stable. The N input

464   rate-GDP per capita relationships also generally fell into the three groups (Fig. 12). But a notable

465   phenomenon is that N input rate in Korea and Japan was much higher than other regions in almost

466   all the three agricultural sectors (Fig. 12). This is also reported by Lim et al. (2021) and they

467   attributed it to decrease of arable land area, high fertilizer input and especially large manure inputs,

468   although fertilizer input in Korea had been considerably reduced. Despite such a diversity of the

469   N use changes in varied socioeconomic circumstances, the N use/N input rate-GDP per capita

470   relationships and the related spatial patterns will be a valuable reference for any future projection

471   of global anthropogenic N inputs.

472
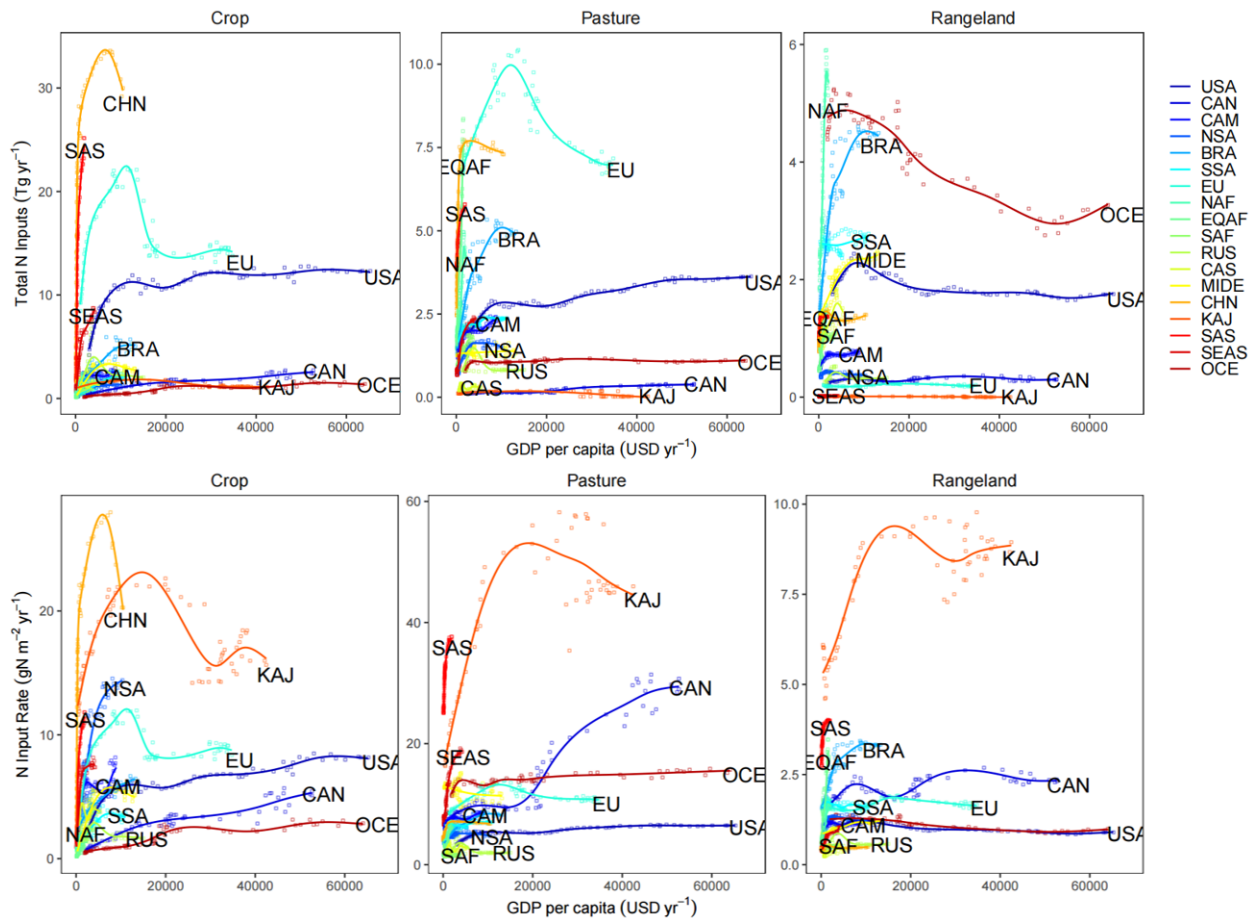
Figure 12. Relationships between total N inputs (excluding N deposition; the top row) or N input rate (the bottom row) and GDP per capita in cropland, pasture and rangeland, respectively, within each of 18 regions during 1961-2019. The lines were fitted using the generalized additive models. For displaying clarity, not all region names are shown in each panel. The 18 regions are USA, Canada (CAN), Central America (CAM), Northern South America (NSA), Brazil (BRA), Southwest South America (SSA), Europe (EU), Northern Africa (NAF), Equatorial Africa (EQAF), Southern Africa (SAF), Russia (RUS), Central Asia (CAS), Middle East (MIDE), China (CHN), Korea and Japan (KAJ), South Asia (SAS), Southeast Asia (SEAS), and Oceania (OCE).

4.2 Implications for nitrogen use management

Excessive N use has induced a variety of environmental issues, due to the magnitude, trend and the constitute forms. In regions or countries like Europe and the US, though the N inputs have been stable (Fig. 12), the large magnitude of annual N inputs results in a considerable fraction of reactive N that is stored in soils. This N pool can cause strong legacy effects, of which the influence on

488 water quality would last for decades (Meter et al., 2018). Therefore, maintaining the current levels

489 of N inputs is far from reducing N related environmental issues in these regions or countries (Liu

490 et al. 2016). Instead, agricultural nitrogen inputs are required to be eliminated drastically, which,

491 however, seems rather difficult at the current technological level even the social-economic

492 conditions are improving (Fig. 12). But for regions or countries like South Asia and Southeast Asia,

493 where N inputs have been increasing rapidly, the management options or activities that are

494 successful in Europe or USA can be promoted to inhibit the further increase of anthropogenic N

495 inputs and local N induced pollution. This requires wide international collaboration and efficient

496 coordination between developing countries and developed countries. As for the changes in N input

497 forms, a signal worth noting is the increasing fraction NH_4^+-N in the global total N inputs (Figs. 7,

498 11, and S1). High NH_4^+-N fraction has contributed significantly to N induced air pollution (Li et

499 al., 2016), and the change of the ratio of NH_4^+-N over NO_3^--N may affect biodiversity (van den

500 Berg et al., 2016) and plant growth (Zhu et al., 2020; Yan et al., 2019). Improved use of NH_4^+-N

501 will benefit both human society and ecosystems.

4.3 Limitations in data development and knowledge gaps

503 The uncertainties and limitations of this global N input dataset are mainly derived from the

504 following aspects: (1) Fixed manure excretion rate. The IPCC Tier 1 method adopts a fixed manure

505 excretion rate for each animal and each country, which can bias the manure production estimate.

506 Although the IPCC Tier 2 method is more realistic in reflecting the dynamic energy intake of

507 livestock (Zhang et al., 2022), its parametrization is more difficult. Meanwhile, to be consistent

508 with manure production estimates by Holland et al. (2005), the IPCC Tier 1 method was adopted

509 in this study. (2) Land use maps. Cropland, pasture, and rangeland distribution maps are critical

510 for the spatialization of N fertilizer and manure application. In the data development process, we

511 constrain N input amount of this dataset with the country-level fertilizer/manure consumption from

512 FAO to ensure the total input consistent, but fertilizer use rate per unit cropland area could be

513 significantly biased if the global data differs a lot from the country-specific data. For example, in

514 the US, the higher cropland acreage in HYDE/LUH2 database, compared with the USDA census,

515 is likely to make fertilizer input rate diluted, which could affect the impact assessment of N inputs

516 (Yu and Lu, 2018). (3) Spatial patterns of fertilizer and manure application and deposition rate.

517 The baseline of crop-specific fertilizer and manure use rates is fixed and has been used to determine

518 the spatial patterns of fertilizer and manure inputs over the study period. This conflicts with the

519   reality of inter-and intra-annual dynamics of crop rotation, annual changes in crop harvested area

520   as well as changes in crop-specific fertilizer use rate over time. An ideal spatially explicit fertilizer

521   input data, in the future, ought to consider the dynamics of crop rotation, individual crop area

522   changes, and crop-specific fertilizer use rate over space and time. In addition, the spatial

523   distribution of livestock has greatly changed with industrialization, which would probably lead to

524   changing spatial distributions of total manure over time, given that manure is not usually

525   transported at large distances. (4) Country-level survey data. The country-level fertilizer and

526   manure data from FAO don't separate N application to cropland and pasture. In this study, we

527   separated fertilizer and manure application to cropland and pasture simply based on constant ratios

528   generated by Lassaletta et al. (2014) and Zhang et al. (2015), which ignored either the temporal or

529   the spatial changes of allocation of fertilizer and manure application to cropland and pasture. (5)

530   Pre-1961 N inputs. Since the country-level fertilizer and manure data are only available after 1961,

531   we assumed the change rates of global manure and fertilizer inputs before 1961 followed the

532   change rates of annual global data reported by Holland et al. (2005). (6) Other N sources to

533   terrestrial ecosystems. In this study, the "anthropogenic N inputs" actually do not exclude the

534   natural source of atmospheric N deposition and do not include legume crop biological N fixation

535   (BNF). Leguminous BNF was the most common nitrogen-containing soil fertility maintenance

536   cropping practice before the widespread use of synthetic fertilizer, and is also used in current

537   organic farming practices (Cherr et al., 2006). According to Herridge et al. (2008), the global

538   legume crop BNF was around 21.5 Tg N yr^{-1} in 2005. Since the HaNi dataset here was developed

539   to serve as inputs for terrestrial biosphere models, N components like BNF, which are simulated

540   using different mechanisms by models, were not included. Nevertheless, a related agricultural BNF

541   database will be much meaningful for deepening our understanding of global N cycling and

542   serving as a benchmark for ecosystem models. To accomplish this, in the future more efforts are

543   required in developing long-term spatial and temporal distribution maps of various crops such as

544   cover crops and legume crops, which are not available at the global scale for now to our knowledge.

545   For future data improvements, we call for advanced N management survey/reporting mechanism

546   to develop fine-scale N consumption or use rate data. For example, the commonly used survey

547   data for the global fertilizer database is country-level consumption amount or crop-specific

548   fertilizer input from IFA and FAO, which smoothed large variations in fertilizer application rate

549   at farm level and sub-national scales. A continuous survey of crop-specific fertilizer and manure

550 use at sub-national scale, development of dynamic global land use data, and crop rotation maps
551 with more precise regional patterns are important for improving the resolution and accuracy of
552 geospatial fertilizer and manure data. Additionally, considering fertilizer and manure application
553 timing in the data is also important for agricultural nutrient management, which relies on the efforts
554 and investigations regarding the fertilizer and manure application behavior at multiple spatial
555 scales.

Data availability

557 The History of Anthropogenic N Inputs (HaNi) dataset is available at
558 https://doi.org/10.1594/PANGAEA.942069 (Tian et al., 2022).

Summary

560 In this work, we developed a global annual anthropogenic N input dataset at 5-arcmin resolution
561 during 1860-2019 by integrating multiple available databases into a uniform framework. This
562 dataset for characterizing the History of anthropogenic N inputs (HaNi) includes major pathways
563 and species of anthropogenic N input to the terrestrial biosphere, such as synthetic fertilizer N use
564 in cropland and pasture, manure N application in cropland and pasture, manure N deposition in
565 pasture and rangeland, and atmospheric N deposition. The TN input to global terrestrial
566 ecosystems raised rapidly since the 1940s due to the widespread usage of synthetic N fertilizer,
567 and the increase started to slow down after 2010. The hotpots of TN inputs shifted from Europe
568 and North America to eastern and southern Asia. The TN inputs in North America, Europe, and
569 East and South Asia were dominated by synthetic fertilizer, while those in Central and South
570 America, Africa, Central, and West Asia, and Oceania were dominated by livestock manure. The
571 N usage varied significantly in different socioeconomic circumstances, but the N use-GDP
572 relationships still could provide a valuable reference for future projection of global anthropogenic
573 N inputs. The HaNi dataset can serve as input data for a wide variety of modeling studies in earth
574 system and its components (land, water, atmosphere and ocean), providing detailed information
575 for the assessment of anthropogenic N enrichment impacts on global N cycling and cascading
576 effects on climate, ecosystem, air and water quality. This data will keep updated in the future.

577

578

Author contributions

H.T. designed this work. Z.B., H.S. and X.Q. performed the study and developed the datasets. N.P. plotted all figures. F.N.T. and G.C. provided the FAO dataset. N.M. provided the crop-specific fertilizer and manure datasets. K.N. provided the fertilizer type dataset. S.P., C.L., and R.X. proposed the methods in the study. All authors contributed to the writing of the manuscript.

Competing interests

The authors declare that they have no conflict of interest.

Acknowledgments

This study has been partly supported by National Science Foundation (Grant numbers: 1903722; 1922687), Andrew Carnegie fellowship Program (Grant No. G-F-19-56910). J.L. acknowledge National Natural Science Foundation of China (Grant no. 41625001), H.S. and X.Q. acknowledge National Key R & D Program of China (grant nos. 2017YFA0604702) and National Natural Science Foundation of China (Grant no. 41961124006). F.N.T. acknowledges funding from FAO regular programme. The views expressed in this publication are those of the author(s) and do not necessarily reflect the views or policies of FAO. K.N. is supported by a project, JPNP18016, commissioned by the New Energy and Industrial Technology Development Organization (NEDO) and a JSPS KAKENHI Grant Number JP18K11672. J.C. is supported by the Fundamental Research Funds for the Central Universities (2021QNA6005). We also thank James Gerber for providing us with the data on crop-specific nitrogen manure application. We especially appreciate the constructive comments and suggestions from Dr. Eduardo Aguilera and Dr. Feng Zhou.

References

Bargu, S., Justic, D., White, J. R., Lane, R., Day, J., Paerl, H., and Raynie, R.: Mississippi River diversions and phytoplankton dynamics in deltaic Gulf of Mexico estuaries: A review, Estuar. Coast. Shelf Sci., 221, 39–52, https://doi.org/10.1016/j.ecss.2019.02.020, 2019.

van den Berg, L. J., Jones, L., Sheppard, L. J., Smart, S. M., Bobbink, R., Dise, N. B., and Ashmore, M. R.: Evidence for differential effects of reduced and oxidised nitrogen deposition on vegetation independent of nitrogen load, Environ. Pollut., 208, 890–897, 2016.

Bian, Z., Tian, H., Yang, Q., Xu, R., Pan, S., and Zhang, B.: Production and application of manure nitrogen and phosphorus in the United States since 1860, Earth Syst. Sci. Data, 13, 515–527, https://doi.org/10.5194/essd-13-515-2021, 2021.

Bouwman, A., Drecht, G., and Van der Hoek, K.: Surface N balances and reactive N loss to the environment from global intensive agricultural production systems for the period 1970–2030, Sci. China Ser. C Life Sci. Chin. Acad. Sci., 48 Suppl 2, 767–79, https://doi.org/10.1007/BF03187117, 2005.

Campbell, B. D. and Stafford Smith, D. M.: A synthesis of recent global change research on pasture and rangeland production: reduced uncertainties and their management implications, Agric. Ecosyst. Environ., 82, 39–55, https://doi.org/10.1016/S0167-8809(00)00215-2, 2000.

Chang, J., Havlík, P., Leclère, D., de Vries, W., Valin, H., Deppermann, A., Hasegawa, T., and Obersteiner, M.: Reconciling regional nitrogen boundaries with global food security, Nat. Food, 2, 700–711, 2021.

Cherr, C. M., Scholberg, J. M. S., and McSorley, R.: Green manure approaches to crop production: A synthesis, Agron. J., 98, 302–319, 2006.

Cui, X., Zhou, F., Ciais, P., Davidson, E. A., Tubiello, F. N., Niu, X., Ju, X., Canadell, J. G., Bouwman, A. F., Jackson, R. B., Mueller, N. D., Zheng, X., Kanter, D. R., Tian, H., Adalibieke, W., Bo, Y., Wang, Q., Zhan, X., and Zhu, D.: Global mapping of crop-specific emission factors highlights hotspots of nitrous oxide mitigation, Nat. Food, 2, 886–893, https://doi.org/10.1038/s43016-021-00384-9, 2021.

Cui, Z., Zhang, H., Chen, X., Zhang, C., Ma, W., Huang, C., Zhang, W., Mi, G., Miao, Y., and Li, X.: Pursuing sustainable productivity with millions of smallholder farmers, Nature, 555, 363–366, 2018.

Dodds, W. K.: Nutrients and the "dead zone": the link between nutrient ratios and dissolved oxygen in the northern Gulf of Mexico, Front. Ecol. Environ., 4, 211–217, https://doi.org/10.1890/1540-9295(2006)004[0211:NATDZT]2.0.CO;2, 2006.

Dong, H., Mangino, J., McAllister, T. A., Hatfield, J. L., Johnson, D. E., Lassey, K. R., and Romanovskaya, A.: Emissions from livestock and manure management., 2006.

Eickhout, B., Bouwman, A. F., and van Zeijts, H.: The role of nitrogen in world food production and environmental sustainability, Agric. Ecosyst. Environ., 116, 4–14, https://doi.org/10.1016/j.agee.2006.03.009, 2006.

Eyring, V., Lamarque, J.-F., Hess, P., Arfeuille, F., Bowman, K., Chipperfiel, M. P., Duncan, B., Fiore, A., Gettelman, A., and Giorgetta, M. A.: Overview of IGAC/SPARC Chemistry-Climate Model Initiative (CCMI)

638 community simulations in support of upcoming ozone and climate assessments, SPARC Newsl., 40, 48–
639 66, 2013.

640 Friedlingstein, P., O'sullivan, M., Jones, M. W., Andrew, R. M., Hauck, J., Olsen, A., Peters, G. P., Peters,
641 W., Pongratz, J., and Sitch, S.: Global carbon budget 2020, Earth Syst. Sci. Data, 12, 3269–3340, 2020.

642 Galloway, J. N., Aber, J. D., Erisman, J. W., Seitzinger, S. P., Howarth, R. W., Cowling, E. B., and Cosby, B.
643 J.: The nitrogen cascade, Bioscience, 53, 341–356, 2003.

644 Galloway, J. N., Bleeker, A., and Erisman, J. W.: The Human Creation and Use of Reactive Nitrogen: A
645 Global and Regional Perspective, Annu. Rev. Environ. Resour., 46, 255–288,
646 https://doi.org/10.1146/annurev-environ-012420-045120, 2021.

647 Gilbert, M., Nicolas, G., Cinardi, G., Van Boeckel, T. P., Vanwambeke, S. O., Wint, G. W., and Robinson, T.
648 P.: Global distribution data for cattle, buffaloes, horses, sheep, goats, pigs, chickens and ducks in 2010,
649 Sci. Data, 5, 1–11, 2018.

650 Gruber, N. and Galloway, J. N.: An Earth-system perspective of the global nitrogen cycle, Nature, 451,
651 293–296, https://doi.org/10.1038/nature06592, 2008.

652 Herridge, D. F., Peoples, M. B., and Boddey, R. M.: Global inputs of biological nitrogen fixation in
653 agricultural systems, Plant Soil, 311, 1–18, https://doi.org/10.1007/s11104-008-9668-3, 2008.

654 Holland, E. A., Lee-Taylor, J., Nevison, C., and Sulzman, J. M.: Global N Cycle: fluxes and N2O mixing
655 ratios originating from human activity, ORNL DAAC, 2005.

656 Houlton, B. Z., Almaraz, M., Aneja, V., Austin, A. T., Bai, E., Cassman, K. G., Compton, J. E., Davidson, E.
657 A., Erisman, J. W., Galloway, J. N., Gu, B., Yao, G., Martinelli, L. A., Scow, K., Schlesinger, W. H., Tomich,
658 T. P., Wang, C., and Zhang, X.: A World of Cobenefits: Solving the Global Nitrogen Challenge, Earths
659 Future, 7, 865–872, https://doi.org/10.1029/2019EF001222, 2019.

660 Howarth, R. W.: Coastal nitrogen pollution: A review of sources and trends globally and regionally,
661 Harmful Algae, 8, 14–20, https://doi.org/10.1016/j.hal.2008.08.015, 2008.

662 Hurtt, G. C., Chini, L., Sahajpal, R., Frolking, S., Bodirsky, B. L., Calvin, K., Doelman, J. C., Fisk, J., Fujimori,
663 S., Klein Goldewijk, K., Hasegawa, T., Havlik, P., Heinimann, A., Humpenöder, F., Jungclaus, J., Kaplan, J.
664 O., Kennedy, J., Krisztin, T., Lawrence, D., Lawrence, P., Ma, L., Mertz, O., Pongratz, J., Popp, A., Poulter,
665 B., Riahi, K., Shevliakova, E., Stehfest, E., Thornton, P., Tubiello, F. N., van Vuuren, D. P., and Zhang, X.:
666 Harmonization of global land use change and management for the period 850–2100 (LUH2) for CMIP6,
667 Geosci. Model Dev., 13, 5425–5464, https://doi.org/10.5194/gmd-13-5425-2020, 2020.

668 Klein Goldewijk, K., Beusen, A., Doelman, J., and Stehfest, E.: Anthropogenic land use estimates for the
669 Holocene – HYDE 3.2, Earth Syst. Sci. Data, 9, 927–953, https://doi.org/10.5194/essd-9-927-2017, 2017.

670 Lark, T. J., Spawn, S. A., Bougie, M., and Gibbs, H. K.: Cropland expansion in the United States produces
671 marginal yields at high costs to wildlife, Nat. Commun., 11, 1–11, 2020.

672 Lassaletta, L., Billen, G., Grizzetti, B., Anglade, J., and Garnier, J.: 50 year trends in nitrogen use efficiency
673 of world cropping systems: the relationship between yield and nitrogen input to cropland, Environ. Res.
674 Lett., 9, 105011, https://doi.org/10.1088/1748-9326/9/10/105011, 2014.

675 Li, Y., Schichtel, B. A., Walker, J. T., Schwede, D. B., Chen, X., Lehmann, C. M., Puchalski, M. A., Gay, D. A.,
676 and Collett, J. L.: Increasing importance of deposition of reduced nitrogen in the United States, Proc.
677 Natl. Acad. Sci., 113, 5874–5879, 2016.

678 Lim, J. Y., Bhuiyan, M. S. I., Lee, S. B., Lee, J. G., and Kim, P. J.: Agricultural nitrogen and phosphorus
679 balances of Korea and Japan: Highest nutrient surplus among OECD member countries, Environ. Pollut.,
680 286, 117353, 2021.

681 Liu, J., You, L., Amini, M., Obersteiner, M., Herrero, M., Zehnder, A. J. B., and Yang, H.: A high-resolution
682 assessment on global nitrogen flows in cropland, Proc. Natl. Acad. Sci., 107, 8035–8040,
683 https://doi.org/10.1073/pnas.0913658107, 2010.

684 Liu, J., Ma, K., Ciais, P., and Polasky, S.: Reducing human nitrogen use for food production, Sci. Rep., 6,
685 30104, https://doi.org/10.1038/srep30104, 2016.

686 Lu, C. C. and Tian, H.: Global nitrogen and phosphorus fertilizer use for agriculture production in the past
687 half century: shifted hot spots and nutrient imbalance, Earth Syst. Sci. Data, 9, 181, 2017.

688 Lun, F., Liu, J., Ciais, P., Nesme, T., Chang, J., Wang, R., Goll, D., Sardans, J., Peñuelas, J., and Obersteiner,
689 M.: Global and regional phosphorus budgets in agricultural systems and their implications for
690 phosphorus-use efficiency, Earth Syst. Sci. Data, 10, 1–18, https://doi.org/10.5194/essd-10-1-2018,
691 2018.

692 Melillo, J. M.: Disruption of the global nitrogen cycle: A grand challenge for the twenty-first century,
693 Ambio, 50, 759–763, https://doi.org/10.1007/s13280-020-01429-2, 2021.

694 Meter, K. J. V., Cappellen, P. V., and Basu, N. B.: Legacy nitrogen may prevent achievement of water
695 quality goals in the Gulf of Mexico, Science, 360, 427–430, https://doi.org/10.1126/science.aar4462,
696 2018.

697 Monfreda, C., Ramankutty, N., and Foley, J. A.: Farming the planet: 2. Geographic distribution of crop
698 areas, yields, physiological types, and net primary production in the year 2000, Glob. Biogeochem.
699 Cycles, 22, 2008.

700 Morgenstern, O., Hegglin, M. I., Rozanov, E., O'Connor, F. M., Abraham, N. L., Akiyoshi, H., Archibald, A.
701 T., Bekki, S., Butchart, N., and Chipperfield, M. P.: Review of the global models used within phase 1 of
702 the Chemistry–Climate Model Initiative (CCMI), Geosci. Model Dev., 10, 639–671, 2017.

703 Mueller, N. D., Gerber, J. S., Johnston, M., Ray, D. K., Ramankutty, N., and Foley, J. A.: Closing yield gaps
704 through nutrient and water management, Nature, 490, 254–257, https://doi.org/10.1038/nature11420,
705 2012.

706 Nishina, K., Ito, A., Hanasaki, N., and Hayashi, S.: Reconstruction of spatially detailed global map of NH_4^+
707 and NO_3^- application in synthetic nitrogen fertilizer, Earth Syst. Sci. Data, 9, 149–162,
708 https://doi.org/10.5194/essd-9-149-2017, 2017.

709 Pan, S., Bian, Z., Tian, H., Yao, Y., Najjar, R. G., Friedrichs, M. A. M., Hofmann, E. E., Xu, R., and Zhang, B.:
710 Impacts of Multiple Environmental Changes on Long-Term Nitrogen Loading From the Chesapeake Bay
711 Watershed, J. Geophys. Res. Biogeosciences, 126, e2020JG005826,
712 https://doi.org/10.1029/2020JG005826, 2021.

713 Peñuelas, J. and Sardans, J.: The global nitrogen-phosphorus imbalance, Science, 375, 266–267,
714 https://doi.org/10.1126/science.abl4827, 2022.

715 Potter, P., Ramankutty, N., Bennett, E. M., and Donner, S. D.: Characterizing the Spatial Patterns of
716 Global Fertilizer Application and Manure Production, Earth Interact., 14, 1–22,
717 https://doi.org/10.1175/2009EI288.1, 2010.

718 Rabalais, N. N. and Turner, R. E.: Gulf of Mexico Hypoxia: Past, Present, and Future, Limnol. Oceanogr.
719 Bull., 28, 117–124, https://doi.org/10.1002/lob.10351, 2019.

720 Scheer, C., Pelster, D. E., and Butterbach-Bahl, K.: Editorial Overview: Climate change, reactive nitrogen,
721 food security and sustainable agriculture-the case of N2O, Elsevier, 2020.

722 Schlesinger, W. H. and Bernhardt, E. S.: Biogeochemistry: an analysis of global change, Academic press,
723 2020.

724 Schlesinger, W. H., Reckhow, K. H., and Bernhardt, E. S.: Global change: The nitrogen cycle and rivers,
725 Water Resour. Res., 42, https://doi.org/10.1029/2005WR004300, 2006.

726 Stewart, W. M. and Roberts, T. L.: Food Security and the Role of Fertilizer in Supporting it, Procedia Eng.,
727 46, 76–82, https://doi.org/10.1016/j.proeng.2012.09.448, 2012.

728 Sutton, M. A., Bleeker, A., Howard, C. M., Erisman, J. W., Abrol, Y. P., Bekunda, M., Datta, A., Davidson,
729 E., De Vries, W., and Oenema, O.: Our nutrient world. The challenge to produce more food & energy
730 with less pollution, Centre for Ecology & Hydrology, 2013.

731 Tian, H., Yang, J., Lu, C., Xu, R., Canadell, J. G., Jackson, R. B., Arneth, A., Chang, J., Chen, G., Ciais, P.,
732 Gerber, S., Ito, A., Huang, Y., Joos, F., Lienert, S., Messina, P., Olin, S., Pan, S., Peng, C., Saikawa, E.,
733 Thompson, R. L., Vuichard, N., Winiwarter, W., Zaehle, S., Zhang, B., Zhang, K., and Zhu, Q.: The Global
734 N2O Model Intercomparison Project, Bull. Am. Meteorol. Soc., 99, 1231–1251,
735 https://doi.org/10.1175/BAMS-D-17-0212.1, 2018.

736 Tian, H., Yang, J., Xu, R., Lu, C., Canadell, J. G., Davidson, E. A., Jackson, R. B., Arneth, A., Chang, J., Ciais,
737 P., Gerber, S., Ito, A., Joos, F., Lienert, S., Messina, P., Olin, S., Pan, S., Peng, C., Saikawa, E., Thompson, R.
738 L., Vuichard, N., Winiwarter, W., Zaehle, S., and Zhang, B.: Global soil nitrous oxide emissions since the
739 preindustrial era estimated by an ensemble of terrestrial biosphere models: Magnitude, attribution, and
740 uncertainty, Glob. Change Biol., 25, 640–659, https://doi.org/10.1111/gcb.14514, 2019.

741 Tian, H., Xu, R., Canadell, J. G., Thompson, R. L., Winiwarter, W., Suntharalingam, P., Davidson, E. A.,
742 Ciais, P., Jackson, R. B., Janssens-Maenhout, G., Prather, M. J., Regnier, P., Pan, N., Pan, S., Peters, G. P.,
743 Shi, H., Tubiello, F. N., Zaehle, S., Zhou, F., Arneth, A., Battaglia, G., Berthet, S., Bopp, L., Bouwman, A. F.,
744 Buitenhuis, E. T., Chang, J., Chipperfield, M. P., Dangal, S. R. S., Dlugokencky, E., Elkins, J. W., Eyre, B. D.,
745 Fu, B., Hall, B., Ito, A., Joos, F., Krummel, P. B., Landolfi, A., Laruelle, G. G., Lauerwald, R., Li, W., Lienert,
746 S., Maavara, T., MacLeod, M., Millet, D. B., Olin, S., Patra, P. K., Prinn, R. G., Raymond, P. A., Ruiz, D. J.,
747 van der Werf, G. R., Vuichard, N., Wang, J., Weiss, R. F., Wells, K. C., Wilson, C., Yang, J., and Yao, Y.: A
748 comprehensive quantification of global nitrous oxide sources and sinks, Nature, 586, 248–256,
749 https://doi.org/10.1038/s41586-020-2780-0, 2020a.

750 Tian, H., Xu, R., Pan, S., Yao, Y., Bian, Z., Cai, W.-J., Hopkinson, C. S., Justic, D., Lohrenz, S., Lu, C., Ren, W.,
751 and Yang, J.: Long-Term Trajectory of Nitrogen Loading and Delivery From Mississippi River Basin to the
752 Gulf of Mexico, Glob. Biogeochem. Cycles, 34, e2019GB006475,
753 https://doi.org/10.1029/2019GB006475, 2020b.

754 Tian, H., Bian, Z., Shi, H., Qin, X., Pan, N., Lu, C., Pan, S., Tubiello, F. N., Chang, J., Conchedda, G., Liu, J.,
755 Mueller, N., Nishina, K., Xu, R., Yang, J., You, L., and Zhang, B.: HaNi: A Historical dataset of
756 Anthropogenic Nitrogen Inputs to the terrestrial biosphere (1860-2019),
757 https://doi.org/10.1594/PANGAEA.942069, 2022.

758 Van Grinsven, H. J. M., Spiertz, J. H. J., Westhoek, H. J., Bouwman, A. F., and Erisman, J. W.: Nitrogen use
759 and food production in European regions from a global perspective, J. Agric. Sci., 152, 9–19, 2014.

760 Vitousek, P. M., Aber, J. D., Howarth, R. W., Likens, G. E., Matson, P. A., Schindler, D. W., Schlesinger, W.
761 H., and Tilman, D. G.: Human Alteration of the Global Nitrogen Cycle: Sources and Consequences, Ecol.
762 Appl., 7, 737–750, https://doi.org/10.1890/1051-0761(1997)007[0737:HAOTGN]2.0.CO;2, 1997.

763 Wang, Q., Zhou, F., Shang, Z., Ciais, P., Winiwarter, W., Jackson, R. B., Tubiello, F. N., Janssens-
764 Maenhout, G., Tian, H., Cui, X., Canadell, J. G., Piao, S., and Tao, S.: Data-driven estimates of global
765 nitrous oxide emissions from croplands, Natl. Sci. Rev., 7, 441–452, https://doi.org/10.1093/nsr/nwz087,
766 2020.

767 Ward, B.: The Global Nitrogen Cycle, in: Fundamentals of Geobiology, edited by: Knoll, A. H., Canfield, D.
768 E., and Konhauser, K. O., John Wiley & Sons, Ltd, Chichester, UK, 36–48,
769 https://doi.org/10.1002/9781118280874.ch4, 2012.

770 West, P. C., Gerber, J. S., Engstrom, P. M., Mueller, N. D., Brauman, K. A., Carlson, K. M., Cassidy, E. S.,
771 Johnston, M., MacDonald, G. K., Ray, D. K., and Siebert, S.: Leverage points for improving global food
772 security and the environment, Science, 345, 325–328, https://doi.org/10.1126/science.1246067, 2014.

773 Wu, Y., Xi, X., Tang, X., Luo, D., Gu, B., Lam, S. K., Vitousek, P. M., and Chen, D.: Policy distortions, farm
774 size, and the overuse of agricultural chemicals in China, Proc. Natl. Acad. Sci., 115, 7010–7015, 2018.

775 Xiong, Z. Q., Freney, J. R., Mosier, A. R., Zhu, Z. L., Lee, Y., and Yagi, K.: Impacts of population growth,
776 changing food preferences and agricultural practices on the nitrogen cycle in East Asia, Nutr. Cycl.
777 Agroecosystems, 80, 189–198, 2008.

778 Xu, R., Tian, H., Pan, S., Prior, S. A., Feng, Y., Batchelor, W. D., Chen, J., and Yang, J.: Global ammonia
779 emissions from synthetic nitrogen fertilizer applications in agricultural systems: Empirical and process-
780 based estimates and uncertainty, Glob. Change Biol., 25, 314–326, https://doi.org/10.1111/gcb.14499,
781 2019a.

782 Xu, R., Tian, H., Pan, S., Dangal, S. R. S., Chen, J., Chang, J., Lu, Y., Skiba, U. M., Tubiello, F. N., and Zhang,
783 B.: Increased nitrogen enrichment and shifted patterns in the world's grassland: 1860–2016, Earth Syst.
784 Sci. Data, 11, 175–187, https://doi.org/10.5194/essd-11-175-2019, 2019b.

785 Yan, L., Xu, X., and Xia, J.: Different impacts of external ammonium and nitrate addition on plant growth
786 in terrestrial ecosystems: A meta-analysis, Sci. Total Environ., 686, 1010–1018, 2019.

787 Yu, Z. and Lu, C.: Historical cropland expansion and abandonment in the continental U.S. during 1850 to
788 2016, Glob. Ecol. Biogeogr., 27, 322–333, https://doi.org/10.1111/geb.12697, 2018.

789 Zhang, B., Tian, H., Lu, C., Dangal, S. R. S., Yang, J., and Pan, S.: Global manure nitrogen production and
790 application in cropland during 1860–2014: a 5 arcmin gridded global dataset for Earth system modeling,
791 Earth Syst. Sci. Data, 9, 667–678, https://doi.org/10.5194/essd-9-667-2017, 2017.

792 Zhang, J., Cao, P., and Lu, C.: Half-Century History of Crop Nitrogen Budget in the Conterminous United
793 States: Variations Over Time, Space and Crop Types, Glob. Biogeochem. Cycles, 35, e2020GB006876,
794 https://doi.org/10.1029/2020GB006876, 2021a.

795 Zhang, L., Tian, H., Shi, H., Pan, S., Chang, J., Dangal, S. R. S., Qin, X., Wang, S., Tubiello, F. N., Canadell, J.
796 G., and Jackson, R. B.: A 130-year global inventory of methane emissions from livestock: Trends,
797 patterns, and drivers, Glob. Change Biol., 28, 5142–5158, https://doi.org/10.1111/gcb.16280, 2022.

798 Zhang, X., Davidson, E. A., Mauzerall, D. L., Searchinger, T. D., Dumas, P., and Shen, Y.: Managing
799 nitrogen for sustainable development, Nature, 528, 51–59, https://doi.org/10.1038/nature15743, 2015.

800 Zhang, X., Zou, T., Lassaletta, L., Mueller, N. D., Tubiello, F. N., Lisk, M. D., Lu, C., Conant, R. T., Dorich, C.
801 D., Gerber, J., Tian, H., Bruulsema, T., Maaz, T. M., Nishina, K., Bodirsky, B. L., Popp, A., Bouwman, L.,
802 Beusen, A., Chang, J., Havlík, P., Leclère, D., Canadell, J. G., Jackson, R. B., Heffer, P., Wanner, N., Zhang,
803 W., and Davidson, E. A.: Quantification of global and national nitrogen budgets for crop production, Nat.
804 Food, 2, 529–540, https://doi.org/10.1038/s43016-021-00318-5, 2021b.

805 Zhu, X., Yang, R., Han, Y., Hao, J., Liu, C., and Fan, S.: Effects of different NO 3−: NH 4+ ratios on the
806 photosynthesis and ultrastructure of lettuce seedlings, Hortic. Environ. Biotechnol., 61, 459–472, 2020.

807